Membrane protein structure from rotational diffusion ☆

Bibhuti B. Das, Sang Ho Park, Stanley J. Opella *

Department of Chemistry and Biochemistry, University of California San Diego, La Jolla, CA 92093-0307 USA

ARTICLE INFO

ABSTRACT

The motional averaging of powder pattern line shapes is one of the most fundamental aspects of sold-state NMR. Since membrane proteins in liquid crystalline phospholipid bilayers undergo fast rotational diffusion, all of the signals reflect the angles of the principal axes of their dipole–dipole and chemical shift tensors with respect to the axis defined by the bilayer normal. The frequency span and sign of the axially symmetric powder patterns that result from motional averaging about a common axis provide sufficient structural restraints for the calculation of the three-dimensional structure of a membrane protein in a phospholipid bilayer environment. The method is referred to as rotationally aligned (RA) solid-state NMR and demonstrated with results on full-length, unmodified membrane proteins with one, two, and seven trans-membrane helices. RA solid-state NMR is complementary to other solid-state NMR methods, in particular oriented sample (OS) solid-state NMR of stationary, aligned samples. Structural distortions of membrane proteins from the truncations of terminal residues and other sequence modifications, and the use of detergent micelles instead of phospholipid bilayers have also been demonstrated. Thus, it is highly advantageous to determine the structures of unmodified membrane proteins in liquid crystalline phospholipid bilayers under physiological conditions. RA solid-state NMR provides a general method for obtaining accurate and precise structures of membrane proteins under near-native conditions. This article is part of a Special Issue entitled: NMR Spectroscopy for Atomistic Views of Biomembranes and Cell Surfaces. Guest Editors: Lynette Cegelski and David P. Weliky.

© 2014 Elsevier B.V. All rights reserved.

1. Introduction

Proteins are responsible for the vast majority of biological functions. Understanding the mechanisms by which these functions are carried out necessarily begins with the three-dimensional structures of the proteins. The history of protein structure determination is relatively short. Starting around 1960, X-ray crystallography [1,2], solution NMR [3], and solid-state NMR [4] have provided detailed descriptions of the structures of one class of proteins – highly hydrated globular proteins – in single- or poly- crystalline samples or in aqueous solution. Both magic angle sample spinning (MAS) solid-state NMR of unoriented samples [5] and oriented sample (OS) solid-state NMR [6] have been used to provide the atomic-resolution detail that is also essential for understanding the functions of the non-globular, often insoluble proteins that are constituents of functional supramolecular assemblies [7–9], including virus particles [10], amyloid fibrils [11], and especially membranes [12,13], the principal subject of this article.

Although sample preparation, instrumentation, experimental methods, and calculation methods have advanced since the first high-resolution solid-state NMR spectra of proteins were obtained

around 1980 [6,14]. Only in the last few years [15,16] has it become possible to determine atomic resolution structures of membrane proteins prepared by heterologous expression in their native environment of phospholipid bilayers [17,18]. Somewhat earlier it was possible to determine the structures of membrane associated peptides and proteins in detergent environments by X-ray crystallography and solution NMR, although these structures are accompanied by concerns that they are distorted due to perturbations from the non-native environments [19,20]. Many membrane proteins have had their sequences modified to enhance the feasibility of X-ray crystallography or NMR spectroscopy, however, here too there are concerns about the effects of using non-native peptide sequences on the structures that are determined [21]. The goal, which has been achieved with OS solid-state NMR, is that unmodified membrane proteins in liquid crystalline phospholipid bilayers can have their structures determined under near-native conditions [13,21–26].

Membrane proteins represent one-third of the proteins expressed from a typical genome [27], carry out many unique biological functions, and act as receptors for most drugs used in the practice of medicine. Thus, the fifty-year lag in structure determination of membrane proteins compared to globular proteins is not due to a lack of motivation, but rather it is because it has proven to be much more difficult to experimentally determine their structures. Membrane proteins require a lipid environment for solubilization, folding, and function, and both artificial and natural lipid environments are highly problematic for both X-ray

---

☆ This article is part of a Special Issue entitled: NMR Spectroscopy for Atomistic Views of Biomembranes and Cell Surfaces. Guest Editors: Lynette Cegelski and David P. Weliky.
* Corresponding author.
  E-mail address: sopella@ucsd.edu (S.J. Opella).

crystallography and solution NMR. They interfere with crystallization and slow the reorientation of the proteins in solution. Further, detergents, non-natural phospholipids, and their mixtures form non-native phases that vary substantially from the native liquid crystalline phospholipid bilayer environment of biological membranes, and, as mentioned, present a serious risk of distorting the structures [19,20]. Here we present rotationally aligned (RA) solid-state NMR as a general method of membrane protein structure determination that takes advantage of the properties of phospholipid bilayers to yield atomic resolution structures under near-native conditions [24,28].

It is likely that many of the difficulties encountered in dealing with samples of protein-containing phospholipid bilayers are due to the global motions of the membrane proteins in the bilayers, for example problems in crystallization. However, these motions are fundamental to the nature of biological membranes [29,30]. It may seem counterintuitive, but the presence of global motions, in particular the fast rotational diffusion of the membrane proteins about the bilayer normal, makes it possible to determine the structures of the proteins with RA solid-state NMR [31]. Indeed, the structure is determined from the motion. The structures of several different membrane proteins are presented here, and they suggest paths toward future developments in the field. The fundamental advantages of studying membrane proteins in their native phospholipid bilayer environment under physiological conditions are so great that RA solid-state NMR has the potential to become a standard method for determining the structures of membrane proteins in the future.

The three-dimensional structure of a protein is determined by both its primary structure, the linear sequence of amino acid residues in the polypeptide, and its surrounding chemical environment [32]. These considerations dominate the determination and the analysis of membrane protein structures. Although equally true for all proteins, the influence on protein structure by its environment is most evident in membrane proteins largely because they are embedded in highly asymmetric, liquid crystalline phospholipids, rather than an isotropic aqueous solution or a regular lattice. Membrane proteins require immersion in liquid crystalline phospholipid bilayers in order to fold into their native structure and to function. Solid-state NMR is required for studies of membrane proteins associated with lipid bilayers because they are effectively "immobilized" by their interactions in this large supramolecular membrane complex. A variety of solid-state NMR approaches to studies of membrane proteins have been reviewed [9,15,17,18,33]. The field is fortunate in having an up-to-date web site of the structures of membrane proteins determined by solid-state NMR (http://www.drorlist.com/nmr/MPNMR.html). The structures of proteins obtained by heterologous expression and reconstituted in phospholipids are providing the foundation for the future of the field, since they incorporate the principal advantages of the method. The structures of domains and of full-length membrane proteins determined by oriented sample solid-state NMR of stationary, aligned samples include the M2 channel-lining segment of the acetylcholine receptor [22] (PDB code: 1CEK), the Influenza M2 channel [34] (PDB code: 2LOJ), the membrane-bound form of the coat protein from filamentous bacteriophage fd [13] (PDB code: 1MZT), the transmembrane channel-forming domain of Vpu from HIV-1[23] (PDB code: 1PJE), phospholamban [35], and the truncated form of the mercury transport membrane protein MerFt [36] (PDF code: 2H3O). By combining OS solid-state NMR data with solution NMR data obtained on the same proteins in micelles, there are additional examples of membrane proteins with their structures determined, which include stannin [37] (PDB code: 1ZZA), phospholamban [38] (PDB code: 2KYV), the membrane-bound form of the coat protein from filamentous bacteriophage Pf1 [39] (PDB code: 2KSJ), and cytochrome b5 [40] (PDB code: 2M33). Of greatest relevance to the topic of deriving structure from motion in this article are the membrane protein structures determined by rotationally aligned solid-state NMR, which include the truncated form of the mercury transport

membrane protein MerFt [24] (PDB code: 2LJ2), the full-length mercury transport membrane protein MerF [21] (PDB code: 2M67), the 350-residue chemokine receptor CXCR1 [25] (PDB code: 2LNL), and the viral membrane protein p7 from the human hepatitis C virus.

Proteoliposomes are nearly ideal samples for structure determination of membrane proteins because it is likely that the forces exerted on the polypeptides are similar to those of biological membranes. Significantly, the proteins in phospholipid bilayers are highly constrained in most directions while undergoing two types of large-amplitude, rapid, global motions — rotational diffusion about the bilayer normal and lateral diffusion in the plane of the bilayer. Most previous characterizations of membrane protein dynamics have focused on local backbone and side chain motions, many of which have important implications for the functions of the proteins [41–43], but are not of direct relevance to the structure determination made possible by the global rotational diffusion of the proteins. NMR is generally insensitive to translation motions and they do not affect the data used for structure determination.

RA solid-state NMR of membrane proteins [21,24,25,28,44] can be summarized in terms of five steps: 1.) Sample preparation; 2.) Resolution of individual resonances; 3.) Assignment of resonances to individual protein sites; 4.) Measurement of structural restraints for individual protein sites; and 5.) Calculation of the protein structures from the structural restraints derived from the experimental solid-state NMR data. Here we focus on the steps that have the strongest influence on the success of the method. These are the expression, purification, refolding, and sample preparation of a membrane protein such that it undergoes rapid rotational diffusion about the normal of phospholipid bilayers, and the NMR experimental methods that provide the resolution, assignment, and measurement of structural restraints for individual protein sites. Perhaps two-thirds of the overall effort is devoted to molecular biology and biochemistry for sample preparation. It is essential that the protein is extremely pure, properly folded, and in a detergent-free phospholipid bilayer environment. Even small amounts of detergents left over from purification and refolding procedures can destabilize and distort the structure of a membrane protein.

RA solid-state NMR exploits the influence of global rotational diffusion of the membrane proteins about the bilayer normal [29,45, 46] for protein structure determination. The first steps are to prepare a sample of a uniformly ^{13}C and ^{15}N labeled membrane protein in liposomes; use MAS solid-state NMR to demonstrate that the protein is undergoing rapid rotational diffusion under the experimental conditions used for structure determination [24,31,47], resolve and partially assign signals with two-dimensional homo- and heteronuclear correlation spectroscopy, and then obtain complete assignments with three-dimensional chemical-shift [24] and dipolar coupling [48] based experiments.

Although the initial spectra are obtained on a protein that is not undergoing rapid diffusional motion, subsequent measurements require that the protein undergo this characteristic global motion. Thus, it is necessary to ensure that the protein is undergoing fast rotational diffusion about the bilayer normal under the experimental conditions used to measure the structural restraints. The bulk of the experimental NMR measurements are used to obtain multiple orientational restraints from motionally averaged powder pattern line shapes. Distance measurements provide valuable complementary data. The final step is to calculate the protein structures using the experimental data as structural restraints.

Well-understood physical laws, two of which are directly pertinent to determining structure from global motions, govern NMR spectroscopy. One is the timescale defined by the operative nuclear spin interactions. The frequency breadth of the spin-interactions, as represented by the span of the powder patterns, defines a "ruler" for the rate at which motions affect the spectra. Motions that are 'fast' compared to the frequency breadth average the powder patterns in a characteristic manner, and those that are 'slow' do not affect the spectra. The

second is the angular dependence, which has an equally strong, but completely different effect on the line shapes of the powder patterns [49].

The first surprise of NMR spectroscopy was finding a doublet, shown in Fig. 1A, instead of a single broad line for a solid sample. The Pake powder pattern doublet from two proximate nuclei provided structural information as early as 1948 [50], namely an unambiguous measurement of the internuclear distance. More complex spectral patterns result from larger groups of spins, and both angles and distances could be deduced from the shape and breadth of the resulting powder patterns [51]. Also, dramatic differences were observed between single- and poly-crystalline samples [50]. In single crystals, the dipole–dipole coupling manifests itself as splittings of single lines, and its magnitude depends both on distance between the nuclei and angles between the internuclear vectors and the magnetic field. By itself, this was sufficient to establish solid-state NMR as a method of determining molecular structures. In the current generation of structural studies, the internuclear distances are generally known and fixed, such C–H and N–H bonds, and the magnitudes of the dipolar couplings are dependent on the angles of the bonds with respect to the axis of alignment [52]. With a sufficient number of bond angles, it is possible to calculate the three-dimensional structure of the protein [53,54]. Additional information in the form of isotropic chemical shifts and distance measurements is helpful, but with a fully rigid backbone, angles alone are sufficient to calculate the three-dimensional structure.

Another surprise at the beginning of solid-state NMR spectroscopy was the effect of motion on the spectra [49]. First there was the finding that there were substantial molecular motions in seemingly rigid solids that strongly affected the NMR spectra. Second was the finding that it wasn't a generalized narrowing, but rather well-defined motions about a single axis produced predictable and quantitative changes in the powder patterns that could be directly related to the line shapes observed in the same samples without motions, for example at very low temperatures. This is illustrated in Fig. 1 for both the dipole–dipole and chemical shift anisotropy spin interactions. The comparison between the calculated Pake doublets in Fig. 1A shows the effect of 180° motion on the powder pattern that results from the coupling of two spin S = ½ nuclei [49]. Similarly, the overlay of "low" and "high" temperature spectra in Fig. 1B shows that at low temperature a methyl group has a relatively broad, non-axially symmetric chemical shift powder pattern, but that when the temperature is raised sufficiently to induce motion about the tetrahedral bond axis, a narrower axially symmetric powder pattern results [55]. Notably, the motionally averaged powder patterns in Fig. 1 reflect the precise geometry of the internal motion about a fixed axis in unoriented polycrystalline samples. They are highly relevant to the situations encountered with proteins used as samples for $^1H/^{13}C/^{15}N$ triple-resonance experiments. This is the key concept for deriving structural information from rotationally averaged powder patterns. In the case of membrane proteins, we assume, and check experimentally, that the backbone N–H and C–H bonds are rigid on the time scales of the dipole-dipole and chemical shift interactions; thus, it is only the global rotational diffusion of the protein in the liquid crystalline bilayer that averages the powder pattern, as determined by the angle between the principal axis of the coupled pair of nuclei or the chemical shift tensor of a site.

With the increasing interest in the analysis of the functions of membrane proteins in terms of their structures, there is a heightened concern about the influence of the surrounding environment when it is provided by detergents, non-natural lipids, organic solvents, crystal packing, *etc.* [19,20]. Nonetheless, considerable progress has been made in describing the structures of membrane proteins, primarily by focusing on exceptional cases, for example bacteriorhodopsin. The early applications of electron microscopy of tilted, unstained samples to identify the seven trans-membrane helices of bacteriorhodopsin in its native purple membrane environment were important first steps in understanding the architecture of membrane proteins [56]. As shown by a variety of experimental measurements, bacteriorhodopsin molecules are constrained in their highly ordered bilayer environment containing diphytanyl lipids. However, when the protein is purified and reconstituted into bilayers consisting primarily of phosphatidyl choline lipids, it undergoes rapid rotational diffusion about the bilayer normal at temperatures above the gel to liquid crystalline phase transition temperature of the lipids, as illustrated in Fig. 2 [43]. The spectrum in Fig. 2B is of bacteriorhodopsin at 3 °C, well below the DMPC phase transition temperature. The chemical shift powder pattern from the carbonyl carbons has the full width and asymmetry expected in a rigid lattice. In contrast, the spectrum of the same sample obtained at 30 °C (Fig. 2C and D), above the phase transition temperature, is much narrower and axially symmetric as the result of the motional narrowing from the rotational diffusion about the bilayer normal. This shows that the majority of labeled carbonyl groups are aligned in the protein with the C–O bond close to parallel to the bilayer normal, which is consistent with the arrangement of helices in the static structures.

Taken together, these early structural and dynamic studies of bacteriorhodopsin demonstrated that fast rotational diffusion of membrane proteins about the bilayer normal depends on lipid composition and temperature. Typically, the rate of rotational diffusion about the bilayer normal can be switched between frequencies that are "slow" or "fast" on the relevant NMR timescales that are defined by the frequency breadth of the static powder patterns by changing the temperature between values that are below or above, respectively, the gel to liquid crystalline phase transition temperature of the
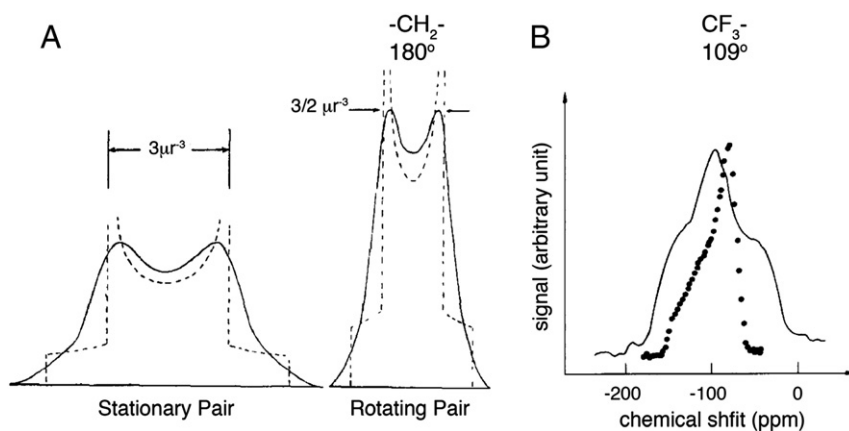

Fig. 1. Motional averaging of powder patterns. A. ^1H–^1H dipole–dipole powder patterns (Pake doublets) for two proximate ^1H nuclei that are stationary (left) or undergoing 180° internal motion (right) [49]. B. ^{19}F chemical shift powder patterns of silver trifluoroacetate at 107 K (dark dots) and 40 K (solid line). The spectra are characteristic of rotating (107 K) and rigid (40 K) CF$_3$ groups [55].
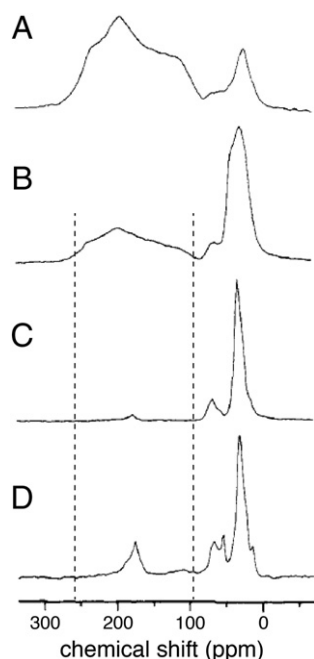
Fig. 2. ^{13}C NMR powder spectra of samples of ^{13}C′-leucine-labeled bacteriorhodopsin (bR) [43]. The carbonyl carbon resonances are centered on 175 ppm and the aliphatic resonances are in the region 20 ppm–80 ppm. A. Hydrated native purple membrane at 3 °C. B. Reconstituted bR-containing DMPC bilayer vesicles at 3 °C. C. Same as in "B." except at 30 °C. D. Same as in "C." where the spectrum was obtained with a Hahn echo sequence. The vertical dashed lines mark the discontinuities of the rigid lattice carbonyl carbon chemical shift powder pattern. Fig. 2 is reprinted with permission from the American Chemical Society, copyright 1985 [43].

Fig. 3. Cartoon representation of the fluid mosaic model of biological membranes [58]. The arrows indicate the rotational diffusion of the proteins about the bilayer normal [44]. Fig. 3 is reprinted with permission from the American Chemical Society, copyright 2013 [44].

phospholipids. These experiments serve to map out the basic parameters of lipid and protein motions in artificial and biological membrane bilayers. Of particular importance to structure determination is the finding that under most conditions even quite large membrane proteins undergo fast rotational diffusion about the bilayer normal [47].

Early studies indicated that membranes were in a 'fluid' state, a term that was often used synonymously with the liquid crystalline state [57]. Certainly some of the magnetic resonance experiments on synthetic and biological bilayers gave results compatible with large amplitude effectively isotropic motions because of the extensive line narrowing. However, as the research moved toward unperturbed bilayers, the asymmetric nature of phospholipid bilayers dominated the effects. This is illustrated in Fig. 3 with a cartoon of rotating membrane proteins in a fluid bilayer adapted from that originally presented as a description of the fluid mosaic model of a membrane by Singer and Nicholson [58]. As mentioned above, early critical experiments utilized rhodopsin, especially those of Cone [45], which measured the relaxation due to rotation about an axis normal to the plane of the disc membrane.

The basic features of mechanical and "rotational alignment" of bilayers were first demonstrated by McLaughlin and coworkers [59] with ^{31}P NMR spectra of oriented and unoriented samples of phospholipids, which themselves undergo rapid rotational diffusion about the bilayer normal. As described above, Griffin and coworkers [43] in Fig. 2 showed that the ^{13}C NMR spectra of unoriented bacteriorhodopsin labeled with ^{13}C in some backbone carbonyl sites could be used to monitor the global rotational diffusion of the protein in unoriented bilayers; at temperatures below the gel to liquid crystalline transition of the lipids the protein is immobile on the relevant NMR timescales and the full frequency span and asymmetry of the carbonyl ^{13}C chemical shift tensor are observed; at higher temperatures the protein undergoes rotational diffusion that is rapid enough to yield a motionally averaged powder pattern with dramatically reduced frequency span. Rhodopsin [45] and CXCR1 [47], which like bacteriorhodopsin have seven trans-membrane helices, undergo rapid rotational
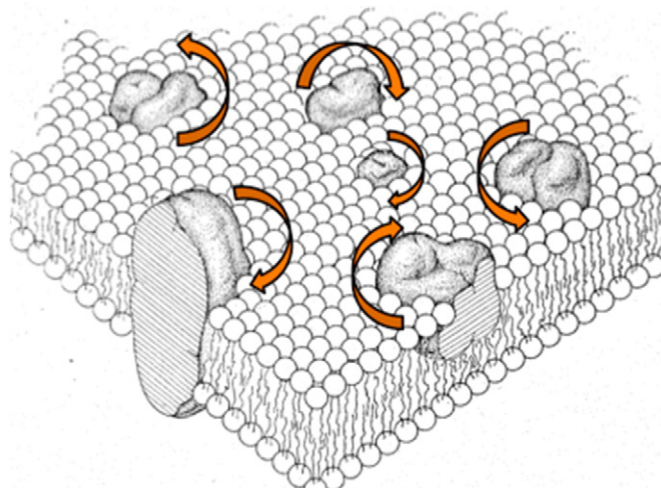
diffusion about the bilayer normal under similar conditions. Even more convincing are 'tilted bilayer' experiments where single-line resonances are observed over the full range of orientations of the bilayer normals with respect to the magnetic field [59,60]. The frequency position of the single line spectra changes as a function of rotation of the proteolipid containing plates for both the ^{31}P NMR spectra of the phospholipids and the ^{15}N NMR spectra of the labeled protein.

As shown in Fig. 4, the protein-containing bilayers are not oriented relative to the magnetic field or the axis of magic angle spinning. Their axis of rotation is defined by the bilayer normal; the global molecular rotation is completely independent of the mechanical rotation of the sample itself.

Studies of small synthetic peptides are not necessarily relevant to those of expressed membrane proteins. However, they have reinforced the concepts of rotational diffusion about the bilayer normal and the consequent motional averaging of powder patterns in unoriented samples. Gramicidin, which exists as a dimer in the membrane, is the archetypical membrane associated peptide [12]. Using specifically ^{13}C′ labeled gramicidin [61] spectra very similar to those of selectively ^{13}C-Leu labeled bacteriorhodopsin [43] were obtained. At temperatures below the gel to liquid crystalline phase transition, full, static chemical shift anisotropy powder patterns were observed for the carbonyl groups in the peptide linkages. In contrast, at temperatures above the transition where the peptide and protein undergo fast rotational diffusion about the bilayer normal, drastically narrowed signals were observed, which were consistent with having a broadened axially symmetric line shape with the intensity centered at a frequency near the principal axis that is nearly parallel to the C–O bond in the peptide plane. With uniformly and specifically ^{15}N labeled gramicidin [62], multiple single-line resonances were observed for an aligned sample of the uniformly labeled peptide (and one line for the specifically labeled sample) and the powder pattern for the uniformly labeled sample showed multiple discontinuities that were consistent with the positions of the single line resonances, thus demonstrating that the angles between ^{1}H–^{15}N bonds and the magnetic field and the bilayer normal, which in this case are collinear, could be measured from either aligned or powder samples. Later, gramicidin was used as an example to demonstrate a distinctive "X" pattern in two-dimensional separated local field spectra, indicating colinearity of the principal axes of the ^{15}N chemical shift and the ^{1}H–^{15}N heteronuclear dipolar coupling interactions, which could only occur with fast rotational diffusion of the labeled gramicidin about the bilayer normal [63]. Subsequently,
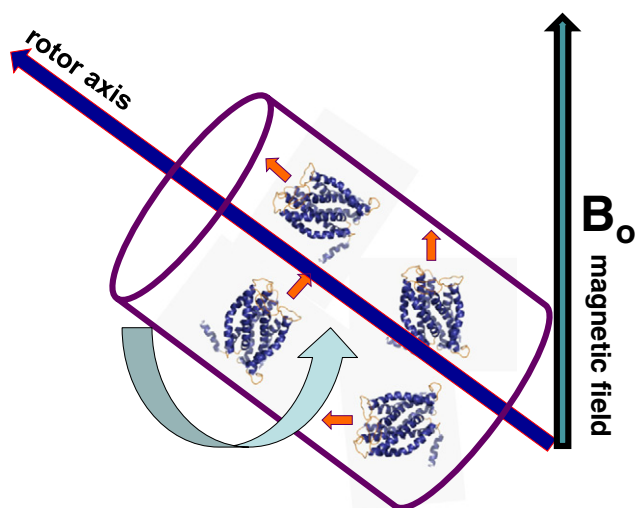
Fig. 4. Cartoon representation of membrane proteins undergoing rotational diffusion about the bilayer normal (orange arrows) in sample in a rotor that is spinning at the magic angle with respect to the magnetic field (blue arrow). The proteins are 'rotationally aligned' along the bilayer normal and not physically or magnetically aligned along the rotor axis of the direction of the magnetic field [31].

specific deuterium labeling was used to further characterize the global reorientation of gramicidin [64].

The rotational diffusion of membrane proteins unifies OS solid-state NMR and MAS solid-state NMR experimental methods (Fig. 4), enabling the complementary use of aligned and unoriented samples, and increasing the potential for synergy between the isotropic and anisotropic nuclear spin interaction approaches to protein structure determination. This is feasible because the same rotationally averaged powder patterns observed in stationary unoriented samples can be measured in MAS solid-state NMR spectra of unoriented samples through the use of multidimensional recoupling experiments [65,66]. We use the spectral parameters associated with the ^{15}N and ^{13}C chemical shifts and ^{1}H–^{15}N and ^{1}H–^{13}C dipolar couplings to determine the orientations of functional groups (chemical shift) or chemical bonds (dipole–dipole coupling) relative to a single axis defined by the direction of the magnetic field or by rotational diffusion about the bilayer normal (in practice, these are the same axis), the protein structure is mapped onto the resulting spectra by the anisotropy of the spin interactions. It is therefore feasible to determine the three-dimensional structure of a protein by relying only on the angular dependence of these spin-interactions, as long as there are no mobile, disordered sections of the polypeptide chain aside from terminal residues.

2. Samples for structure determination

Obtaining milligram amounts of membrane proteins that are isotopically labeled, highly purified, and properly refolded in detergent-free phospholipid bilayers is an essential first step in structure determination by solid-state NMR. This requires an efficient heterologous expression system. It is essential to show that overexpression followed by purification and reconstitution into phospholipid bilayers does not alter the structure or function of the protein. Membranes from prokaryotes and eukaryotes differ in their lipid compositions, which can have a significant effect on the folding and functioning of membrane proteins. Therefore, a thorough characterization of lipid composition is also an essential aspect of sample preparation.

A broad selection of organisms such as bacteria, yeast, insect cells, and mammalian cell cultures, as well as cell-free systems, have been utilized for the recombinant production of membrane proteins. Bacterial expression, especially in *Escherichia coli*, is now sufficiently well developed to provide the high yields of membrane proteins necessary to perform NMR experiments [67]. It can be routinely applied to a range

of membrane proteins [23,68–73]. It offers distinct advantages with respect to simplicity and safety of laboratory procedures, flexibility and cost of isotopic labeling, and the availability of a variety of strains. It provides opportunities for optimization of yield of different membrane proteins and constructs. It also offers well-established methods for genetic manipulation to optimize conditions for expression and purification.

Several of the molecular biology reagents, such as the gene, expression vector, and host cells need to be optimized for overexpression of individual membrane proteins. A very common strategy to express membrane proteins with between one and seven transmembrane helices in *E. coli* is the use of fusion proteins. Functional membrane proteins have been successfully expressed using the N-terminal fusion to the *E. coli* maltose-binding protein (MBP) that targets the protein to the periplasmic membrane [70,74]. The disadvantage of this approach is that toxic effects associated with membrane insertion of large amounts of heterologously overexpressed proteins often limit cell growth. To overcome this problem membrane proteins can be fused to ketosteroid isomerase (KSI) [23,69], Bcl-XL [73], TrpΔLE [68] or glutathione S-transferase (GST) [71], which improve expression levels by targeting the expressed protein to inclusion bodies. Each of these systems has its own advantages and disadvantages, and the choice of the optimal expression system is often empirical. The principal disadvantage of this approach is that proteins expressed in bacterial inclusion bodies have to be refolded, however, after considerable development this can now be accomplished using a standardized approach. Yields of 2–20 mg of final, purified protein per liter of cell culture are obtainable.

G-protein coupled receptors (GPCRs) are of particular interest because of their biological roles in signaling and as drug receptors. Using *E. coli* based expression systems, many GPCRs have been successfully expressed, purified, and refolded [75–78]. Importantly, fully functional proteoliposomes of GPCRs [71] have been obtained. Expression in *E. coli* enabled selective and uniform isotopic labeling with ^{2}H, ^{13}C, and ^{15}N in various combinations. Several critical refinements of the expression, purification, and refolding procedures led to the preparation of highly purified, completely monomeric proteoliposome samples that are stable for many months at 35 °C while subject to the high power radiofrequency irradiations of solid-state NMR experiments [25].

In order to express the chemokine receptor CXCR1 in *E. coli*, the gene encoding unmodified human CXCR1 was cloned into a pGEX vector (www.gelifescience.com) for expression of a GST-CXCR1-His6 fusion protein with GST and CXCR1 linked by a thrombin cleavage sequence, and a six-histidine sequence tag inserted at the C-terminus of CXCR1 to facilitate purification by metal affinity chromatography (Fig. 5A). The fusion protein was expressed in *E. coli* BL21 cells under control of a *tac* promoter. In a typical batch preparation, cultures are initiated by inoculating 50 mL of LB medium, containing 50 mg/L of carbenicillin, with a single bacterial colony grown after transformation. The culture is grown overnight at 37 °C by shaking (180 rpm). The following morning, 10 mL of the overnight pre-culture is used to inoculate 500 mL of M9 minimal medium, containing 1 g/L ^{15}N labeled ammonium sulfate as the sole nitrogen source, 2 g/L of ^{13}C$_6$-glucose as the sole carbon source, plus 50 mg/L of carbenicillin, and bacteria are grown by shaking (150 rpm) at 37 °C, until the OD$_{600}$ reached 0.5. Expression of GST-CXCR1-His6 is induced by adding 80 μM Isopropyl β-D-1-thiogalactopyranoside (IPTG) and growing for an additional 4 h. The concentration of IPTG was optimized to obtain the highest expression and cell growth. Cells are harvested by centrifugation (12,000 × *g*, 15 min, 4 °C) and then stored at −80 °C before lysis.

The development of protocols for the expression and purification of full-length unmodified CXCR1 sets the stage for the preparation of a variety of its truncated constructs to help dissect the biological roles of various domains (Fig. 5B–L). These constructs assist in the studies of the dynamics of CXCR1 [47] and its interactions with the chemokine Interleukin-8 [79].
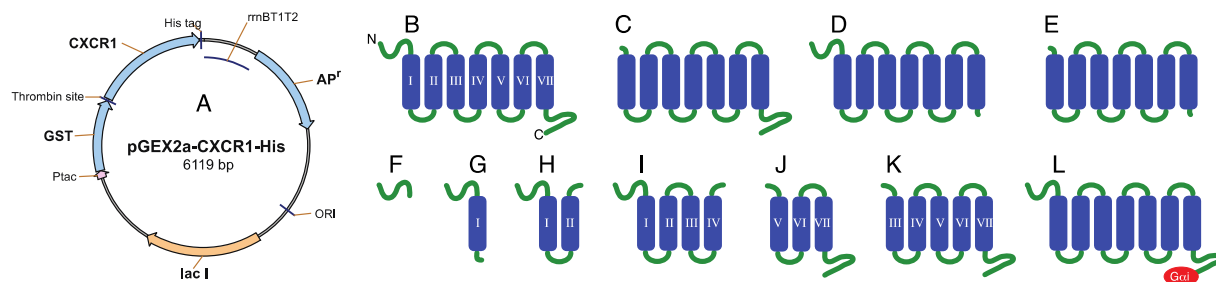
Fig. 5. A. Map of expression vector for CXCR1. The CXCR1 gene is inserted after the GST to express as a GST–CXCR1 fusion protein and the thrombin cleavage site is located between GST and CXCR1 [71]. (B.–L.) Various CXCR1 constructs expressed using the *E. coli* fusion expression system: B. wild-type protein, 1–350; C. N-terminal truncated protein, 39–350; D. C-terminal truncated protein, 1–319; E. N- and C-terminal truncated protein, 23–319; F. N-terminal domain, 1–38; G. N-terminal 1 TM domain, 1–72; H. N-terminal 2TM domain, 1–105; I. N-terminal 4TM domain, 1–192; J. C-terminal 3TM domain, 193–350; K. C-terminal 5TM domain, 106–350; L. Gai peptide (QFVFDAVTDVIIKNNLKDCGLF) fused to the C-terminus of the wild-type protein.

2.1. Isotope labeling strategy

Increasing the sensitivity and resolution of triple resonance solid-state NMR experiments can be accomplished through several strategies: use of higher magnetic fields; improvement of the NMR hardware; new pulse sequence design; non uniform sampling (NUS) of data; and tailoring the isotopic labeling of the NMR samples to facilitate all of these. As larger membrane protein systems are studied, overlap of NMR resonances becomes more problematic, even in three-dimensional experiments. Isotopic labeling schemes can be designed to simplify spectra, guide assignments, and increase the efficiency of spectroscopic techniques by eliminating unwanted spin–spin interactions. Isotopic labeling can be tailored to alter the spectroscopic NMR relaxation properties of a sample. Specific labeling schemes tailored for triple-resonance multidimensional NMR have proven to be highly successful both in solution NMR and solid-state NMR.

A suite of triple-resonance ^{1}H/^{15}N/^{13}C NMR experiments applicable to ^{13}C and ^{15}N labeled proteins without the need for homonuclear ^{13}C–^{13}C decoupling has been developed, even in the case of stationary, aligned samples [80,81]. This was made possible by applying two different patterns of isotopic labeling for ^{13}C and ^{15}N labeled proteins. In one case, the proteins were 100% uniformly ^{15}N labeled in all nitrogen sites, and 20%–40% randomly labeled with ^{13}C in all backbone and side chain sites. The requirement for homonuclear ^{13}C–^{13}C decoupling while detecting ^{13}C signals was avoided because of the low probability of any two ^{13}C being bonded to each other. In another type of samples, minimal media with [2-^{13}C]-glycerol and [1,3-^{13}C]-glycerol as the sole bacterial carbon source and ^{15}N ammonium sulfate as the nitrogen source can be prepared. The [2-^{13}C]-glycerol and [1,3-^{13}C]-glycerol samples displayed complementary patterns of carbon labeling [4]. The use of ^{13}C random isotopic dilution and of metabolic precursors for selective ^{13}Cα and ^{13}C′/^{13}C$_{aliphatic}$ carbons is now routinely applied, and it has been applied to study the dynamics and the structure of CXCR [25,47]. These studies are an important base for future NMR applications because of the use of metabolic precursors for labeling depends on the organism's specific metabolic pathway. It has been applied to grow colonies of *Pseudomonas aeruginosa*, which were subsequently infected with Pf1 bacteriophage to produce labeled bacteriophage coat proteins. This work, together with that of Goldbourt and McDermott [82], who used [1-^{13}C]-glucose as metabolic precursor, opened the door for future applications of site-directed selective labeling of other membrane proteins grown in *P. aeruginosa*, an organism that can potentially provide high yields of ^{2}H labeled protein when grown in D$_2$O [83].

Full three-dimensional structures of membrane proteins require the introduction of triple resonance experiments to study side chains. Only six of the amino acids found in proteins have methyl groups in their side chains (alanine, valine, leucine, isoleucine, methionine, threonine). However, they contribute 35%–40% of the residues in proteins [27]. Since valine, leucine and isoleucine each contain two methyl groups, there are typically 60 methyl groups present in every 100 residues of a protein. Both stationary sample solid-state NMR and magic angle spinning solid-state NMR have been used to characterize ^{13}C–^{1}H couplings in 3-^{13}C-Ala labeled samples [84]. The measurement of heteronuclear dipolar couplings for individual methyl groups in both aligned and unoriented samples lays the foundation for a general approach to complete structure determination that includes backbone and side chain sites.

2.2. Purification

Efficient and rapid purification of monodisperse membrane proteins is essential in order to obtain stable samples. A fusion protein ensures that the overexpressed polypeptide is sequestered in inclusion bodies, which protect the cell membranes from protein overload, and simplifies protein purification. After isolation of the inclusion bodies, the solubilized polypeptide is subjected to nickel affinity chromatography and enzymatic cleavage on the column. Final purification of proteins by size exclusion fast protein liquid chromatography (SEC-FPLC) yields a single band on polyacrylamide gel electrophoresis. Protein aggregation can be reduced by minimizing the exposure of target proteins to detergents during purification before reconstituting into phospholipid bilayers, enabling the high yield and purity of the target membrane proteins.

The protocol for the preparation of membrane proteins is outlined in Fig. 6. It takes 3 days from the bacterial culture to the final NMR sample: day 1, growth of *E. coli* culture and preparation of inclusion bodies; day 2, purification and refolding; day 3, preparation of proteoliposomes and the final NMR sample. The sample purity at each step is monitored by SDS-PAGE (Fig. 6B and C). The final purification by liquid chromatography yields pure proteins, as shown in lane 5 of Fig. 6B and C. The protein purity was shown to be >98% by gel quantification analysis (http://rsb.info.nih.gov/ij/).

Since GPCRs are of particular interest, we provide details of CXCR1 purification. Harvested cells are suspended in 30 mL of lysis buffer (20 mM Tris-HCl, 500 mM NaCl, 15% glycerol, pH 8.0) per L of cell culture, and tip sonicated for 10 min on ice (Fisher Scientific Sonic Dismembrator 550, output control 5). Membrane fragments are solubilized by addition of 10 mg/mL of Triton X-100. Then, inclusion bodies, enriched in GST-CXCR1-His6, are isolated by centrifugation (20,000 × *g*, 30 min, 4 °C), solubilized in 30 mL of binding buffer (20 mM Tris-HCl, 500 mM NaCl, 1% SDS, 10 mM imidazole, 0.1% TCEP, pH 8.0), and allowed to bind to Ni-NTA agarose (Qiagen). The pH is adjusted immediately following the addition of TCEP. The column buffer is exchanged by washing with 20 bed volumes of thrombin cleavage buffer (20 mM HEPES, 250 mm NaCl, 0.1% hexadecylphosphocholine, pH 8.0), and the GST fusion partner is removed by adding 1000 units of thrombin and incubating for 2 h at room temperature. The column is then washed with 10 bed volumes of washing buffer (20 mM Tris-HCl, 0.5% dodecylphosphocholine, 50 mM NaCl, 20 mM imidazole, pH 7.3) and CXCR1 is eluted with 3 bed volumes of elution buffer (20 mM HEPES, 0.5% dodecylphosphocholine, 500 mM
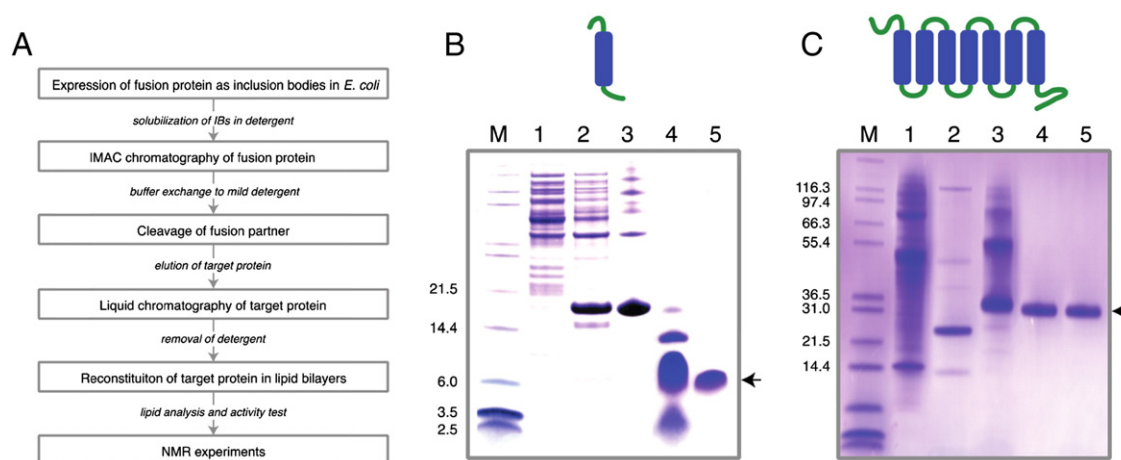
Fig. 6. A. General protocol for preparation of NMR samples of membrane proteins. B. SDS-PAGE analysis of purification procedure of the single transmembrane protein Vpu$_{2-30+}$ [23]: lane 1, discarded supernatant; lane 2, inclusion bodies of the KSI-Vpu$_{2-30+}$ fusion peptide; lane 3, purified fusion peptide from Ni chelate chromatography; lane 4, mixture after CNBr cleavage; lane 5, HPLC purified Vpu$_{2-30+}$. C. SDS-PAGE analysis of purification procedure of the seven transmembrane protein CXCR1 [25]: lane 1, inclusion bodies of the GST-CXCR1 fusion protein; lane 2, flow-through of Ni chelate chromatography; lane 3, CXCR1 from Ni chelate chromatography; lane 4, size exclusion FPLC purified CXCR1; lane 5, CXCR1 proteoliposome after reconstitution.

imidazole, 50 mM NaCl, pH 7.3). Each 10 mL of eluate contains ~5 mg of CXCR1, present primarily as monomer but also as significant amounts of dimer and higher oligomers, as judged by analytical size exclusion chromatography and SDS-PAGE (lane 3 in Fig. 5C). Monomeric CXCR1 is isolated from this mixture by preparative size exclusion chromatography (Superdex 200 HiLoad 26/60 column, GE Healthcare) in column buffer (20 mM HEPES, 0.5% SDS, 50 mM NaCl, pH 7.3). This step yields ~5 mg of monomeric CXCR1. It is important that the CXCR1 samples purified by nickel affinity chromatography that contain a small amount of higher oligomers (Fig. 6C, lane 3) are immediately loaded onto the size exclusion chromatography. Since the trace amount of oligomers (and/or other impurities) apparently facilitate the formation of larger amounts of higher oligomers, any delay between the two chromatography steps reduces the yield of the monomeric protein.

2.3. Refolding to proteoliposomes

The optimized approach for the reconstitution of integral membrane proteins into proteoliposomes relies on the precisely controlled pH and complete removal of the detergent from solutions containing the protein, phospholipids and detergents in excess water [85–87]. The removal of the detergent, which is included initially to solubilize the hydrophobic membrane proteins, is essential for forming stable bilayers, and must be performed in a precise and quantitative manner to avoid the formation of undesirable protein oligomers. The purity and homogeneity of the reconstituted protein is of crucial importance for OS solid-state NMR experiments, since the sample alignment in lipid bilayers is strongly dependent on a precise lipid ratio [87,88]. It is noteworthy that the smallest trace of protein oligomers is problematic for the preparation of stable samples. This is not the case for many other proteins, but it certainly is for CXCR1 [87] and presumably other GPCRs.

The final yield of reconstituted protein in liposomes is strongly related to the procedure used to remove the detergent from the refolding mixture of phospholipids, protein, and detergents, as well as the nature of the phospholipids used during the final co-solubilization process. Several techniques for the removal of detergents have been developed. The choice of the appropriate technique is primarily dependent on the kinds of detergents being removed. SDS is one of the most commonly used detergents for purification of membrane proteins. Three different techniques for the removal of SDS have been compared for reconstitution of CXCR1 into DMPC lipid bilayers [87]: adsorption to BioBeads [89]; complexation with methyl-β-cyclodextrin (MbCD) [90]; and

co-precipitation with potassium chloride (KCl) [91]. Mixed micelle solutions are prepared by dissolving the dried 1,2-Dimyristoyl-*sn*-Glycero-3-Phosphocholine (DMPC) with SDS with a final lipid concentration of 10 mg/ml. Purified CXCR1 was then added to the mixed micelle solution at a protein-to-lipid ratio of 1:5 (w/w) and incubated for 1 h at room temperature.

SDS removal by BioBeads is simple and rapid, and provides an alternative to conventional dialysis, especially when dealing with low critical micelle concentration detergents. However, batches of CXCR1-containing proteoliposomes produced with this approach vary significantly in their lipid content with a total phospholipid loss of up to 20%. Similar effects have been observed using non-recycled adsorbent, which excluded altered affinities due to recycling. The lipid composition monitored by HPLC with an evaporative light scattering detector showed the batch wise inconsistency in the protein-containing DMPC liposomes. The reason for the loss of DMPC may be due to non-specific adsorption to BioBeads, which is a known limitation of this method [92]. Although the adsorptive capacity of BioBeads has become more consistent, the total detergent concentration remains difficult to determine. As a result, the total amount of detergent bound to CXCR1 can only be estimated, and this is simply not adequate for the preparation of stable samples for NMR spectroscopy.

The results of gentle reconstitution using either MßCD or KCl to assist in the removal of the detergent during dialysis are similar. MßCD or KCl is slowly dialyzed against ternary solutions of protein, phospholipid, and detergent. While MßCD is applicable to a broad range of detergents containing long acyl chains [93], KCl is suitable only for detergents having sulfate head groups, specifically SDS [94]. In contrast to procedures that used BioBeads, SDS removal by either MßCD or KCl is highly reproducible and yields proteoliposomes without loss of long chain lipids. Care must be taken, since the rapid reconstitution that results from direct addition of MßCD or KCl to the ternary solution can cause protein oligomerization that is observable by SDS-PAGE. The timing of the reconstitution is optimized to minimize protein oligomerization. The ternary solution is first dialyzed overnight against >200-fold excess volume of a buffer to remove the bulk of the SDS, and then dialyzed against a buffer containing the appropriate amount of MßCD with respect to the sample volume overnight, or 20 mM KCl for 6 h to remove any SDS bound to the proteoliposomes. Although both methods give similar results, the KCl co-precipitation method is specific to SDS, easier to setup, and less expensive than the MßCD complexation method.

2.4. Activity

Their environments as well as their amino acid sequences significantly influence the structures and functions of membrane proteins. Notable differences have been found between the structures of membrane proteins determined in non-lipid bilayer mimetics (*e.g.*, detergents) and those determined in lipid bilayers [21,95]. Although *in vitro* functional assay of recombinant membrane proteins using detergent and/or lipid-based system provides useful information in favorable cases, the native phospholipid bilayer is best suited for characterizing their functions and structures. It is, therefore, important to perform the structure determination and functional assays in the same environment using the same protein construct in order to validate the structure determined by NMR.

Activity of many refolded membrane proteins including GPCRs from inclusion bodies produced in *E. coli* has been reported [75,77]. Refolded CXCR1 proteoliposomes were fully functional and indistinguishable from the native receptor as shown in the G–protein activation assay (Fig. 7A) [71]. Signal disappearance of the ligand interleukin-8 (IL-8) upon interaction with CXCR1 proteoliposomes at 1:1 molar ratio demonstrates that CXCR1 is functional under the NMR experimental conditions (Fig. 7B and C) [79]. Strong interaction between repertaxin, an allosteric inhibitor of CXCR1/CXCR2 and CXCR1 in membrane bilayer environments also helps to confirm the activity of refolded CXCR1 (Fig. 7D and E).

Immobilization of membrane proteins can provide direct analytical access to their surface-based functional assays such as ligand binding, receptor clustering, and signal transduction. The heterologous expression of membrane proteins opens the possibility of fusing affinity tags to the proteins, which greatly facilitates not only purification of proteins but also the development of membrane protein functional assays. The fusion tags comprise polyhistidine-metal ion, antibody-antigen, and biotin-streptavidin recognition elements. It has been shown that biotin-streptavidin interactions provide a good basis for efficient immobilization of proteins on a solid surface for surface plasmon resonance (SPR) applications [96,97]. These immobilization methods can be applied to larger membrane proteins such as GPCRs for receptor–ligand interaction studies.

Recently, Grisshammer and cowokers have successfully used nanodiscs for biophysical characterization of membrane proteins including GPCRs [98]. Protein-containing nanodiscs have been introduced as a soluble bilayer environment compatible with many biophysical experiments, including in some cases solution NMR [99]. It has been shown that the diameter of the phospholipid bilayer disc can be adjusted by changing the molar ratio of the phospholipids

and the 14-residue peptide (Ac-DYLKAFYDKLKEAF-NH2) [100]. The large increase in diameter dramatically alters the behavior of the bilayer discs in aqueous solution. Protein nanodisc assemblies undergo isotropic reorientation; in contrast, protein-containing macrodiscs form magnetically alignable bilayers at temperatures above the gel-to-liquid crystalline transition temperature of the phospholipids. Nanodiscs samples have been used for MAS solid-state NMR experiments where the protein-containing nanodiscs were precipitated with PEG 3350 and the pellets were transferred into a MAS rotor [101,102]. RA solid-state NMR experiments on protein-containing macrodisc samples show that proteins retain their ability to undergo fast rotational diffusion about the lipid bilayer normal so that the orientation-dependent frequencies can be measured for structure calculation. Importantly, the macrodisc samples are stable enough to withstand MAS solid-state NMR experiments.

3. NMR spectroscopy

RA solid-state NMR combines the high resolution and ability to systematically assign resonances that accompanies the use of uniformly ^{13}C and ^{15}N labeled proteins in MAS solid-state NMR with the measurement of the powerful and error-resistant angular restraints of OS solid-state NMR. Recent developments in decoupling and recoupling pulse schemes that suspend the averaging effect of magic angle spinning restore the angular reorientation of dipolar vectors and chemical shielding tensors without sacrificing the sensitivity and resolution provided by magic angle spinning; these enable the measurement of the underlying powder patterns associated with each resonance. The frequency span and sign of the axially symmetric line shapes of the powder patterns averaged by rotational diffusion about the bilayer normal provide the structural restraints used to calculate the three-dimensional structures of proteins. These are the central concepts for determining protein structure from motion through the implementation of RA solid-state NMR.

The powder patterns that appear in a second or more typically third dimension in recoupling experiments are either the full static patterns [103,104], if the protein is fully immobilized by its environment, for example at low temperature, or motionally averaged by global motions, such as rotational diffusion about the bilayer normal [43,47], or local motions, such as side chain reorientations [41,105]. The rotationally averaged powder patterns are the source of the structural restraints used to calculate the three-dimensional structures of the proteins in liquid crystalline phospholipid bilayers. The parallel edge of the motionally averaged axially symmetric powder patterns has exactly the same orientationally-dependent frequency as the single line
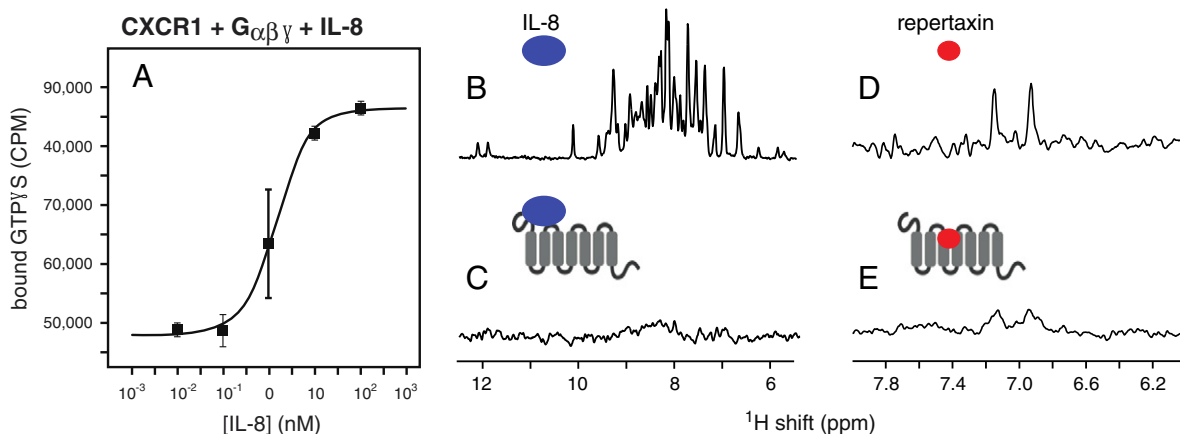

Fig. 7. A. G-protein activation of CXCR1 proteoliposomes. CXCR1 proteoliposomes were reconstituted with $G_{i/o}$ protein trimer and used to measure ^{35}S-labeled GTPγS binding as a function of IL-8 concentration, by measuring radioactivity (CPM) in a scintillation counter [71]. B. and C. ^{15}N edited ^{1}H NMR spectra of B. IL-8 alone and C. complexed with CXCR1. D. ^{1}H NMR spectra of repertaxin alone and E. complexed with CXCR1.

resonance in a uniaxially aligned sample parallel to the direction of the magnetic field, hence the equivalence of RA solid-state NMR and OS solid-state NMR measurements [31].

Cross-polarization (CP) transfer from the "abundant" [1]H nuclei under the Hartmann–Hahn [106] match condition is widely used to enhance the sensitivity of the "dilute" nuclei in the sample, such as ^{13}C and [15]N [107]. Subsequently, decoupling and recoupling techniques are applied to exchange magnetization between spins *via* through-space or through-bond interactions. The polarization transfer techniques often used in multidimensional correlation experiments follow coherence transfer pathways that lead to sequential resonance assignments in proteins. Also, through-bond polarization transfer techniques are available that work efficiently under fast spinning conditions [108].

Separate experiments are usually required to characterize the rigid and flexible regions of proteins. The principal one-dimensional pulse sequences used for characterization of proteins are diagrammed in Fig. 8. The dipolar coupled spins that are rigid on NMR timescales can be observed (Fig. 8D) using the conventional CP-based pulse scheme shown in Fig. 8C. The nuclear spins associated with the flexible regions of the protein are observed (Fig. 8F) using a polarization transfer technique based on J-coupling as diagrammed in the pulse scheme in Fig. 8E. All sites are observed in a spectrum (Fig. 8B) obtained with the direct-excitation pulse sequence diagrammed in Fig. 8A.

The presence of local motions in otherwise immobilized proteins can be readily identified by comparing the results of the one-dimensional experiments diagrammed in Fig. 8. However, in MAS solid-state NMR experiments, the conventional CP pulse sequence diagrammed in Fig. 8C may be inefficient for molecules undergoing global and local motion at intermediate NMR timescales. Some membrane proteins in a phospholipid bilayer environment undergo motion at an intermediate time scale; consequently, they have slow CP transfer rates because the motion interferes with dipolar couplings and radiofrequency irradiations. The motion also shortens the rotating frame relaxation time [109], which adds further complexity to the spin dynamics [110]. However, [1]H-^{13}C nuclear Overhauser polarization (NOP) [111] can be used to enhance the magnetization by up to a factor of two in the presence of motion [112]. This can be achieved by creating a dipolar bath with radio frequency (RF) pulses applied to the ^{1}H nuclei under dipolar assisted rotational resonance (DARR) [113], then establishing contact with the "dilute" nuclei of interest. A pulse sequence that

incorporates this combination of experiments is diagrammed in Fig. 8A. The Overhauser effect transfers magnetization quantitatively to all ^{13}C nuclei with the same dynamic properties. The one pulse ^{1}H decoupled spectrum with NOP records signals from all ^{13}C nuclei irrespective of RF amplitude. The nuclei in the rigid core region and flexible terminal parts of the protein are separately observed using the Hartmann–Hahn CP [114] and Insensitive Nuclei Enhanced by Polarization Transfer (INEPT) [115] techniques, respectively. Signals from about 310 residues contribute in the spectrum shown in Fig. 8D and from about 40 residues in the mobile N and C termini in the spectrum in Fig. 8F.

The resolution and assignment of individual resonances is accomplished by performing multi-dimensional MAS solid-state NMR correlation experiments. [13]C detection provides higher sensitivity and better chemical shift resolution compared to ^{15}N detection, which is typically used in OS solid-state NMR of stationary, aligned samples, and is a major advantage of using uniformly ^{13}C labeled samples and relying on the magic angle spinning to suppress the homonuclear ^{13}C/^{13}C dipolar couplings that are costly to resolution. Two-dimensional ^{13}C/^{13}C correlation spectra of a polypeptide that corresponds to the trans-membrane helical domain of the membrane protein Vpu from HIV [23] are shown in Fig. 9B and C for two different durations of the exchange period. The correlations among the ^{13}C sites are established using the pulse sequence shown in Fig. 9A. Generation of ^{13}C magnetization by conventional CP is followed by isotropic chemical shift evolution with heteronuclear ^{1}H and ^{15}N decoupling. Spin exchange between ^{13}C sites occurs during the mixing period designated by the dotted lines in Fig. 9A. The spectra in Fig. 9 were obtained using proton driven spin diffusion (PDSD) [116,117] (Fig. 9B) and DARR [113] (Fig. 9C) mixing. During the final step, isotropic ^{13}C chemical shift frequencies are detected under heteronuclear decoupling [118,119]. The cross peaks that appear in the two-dimensional spectra provide resolution and enable the signals to be readily identified by residue type. As an example, in Fig. 9B, single-site resolution for Trp, Ala, Ile, and Val residues is illustrated with guidelines following the cross-peaks observed for their side chain signals. [13]C/^{13}C correlations within a residue are typically observed using a short mixing period of about 50 ms for PDSD or about 20 ms for DARR. The correlations in inter-residue and inter-molecular contacts over large distances can be observed with longer mixing period of up to 500 ms for PDSD and 200 ms for DARR. As an example, the dotted box in red in Fig. 9C illustrates guidelines for inter-residue contacts with [13]CA/[13]CA correlation
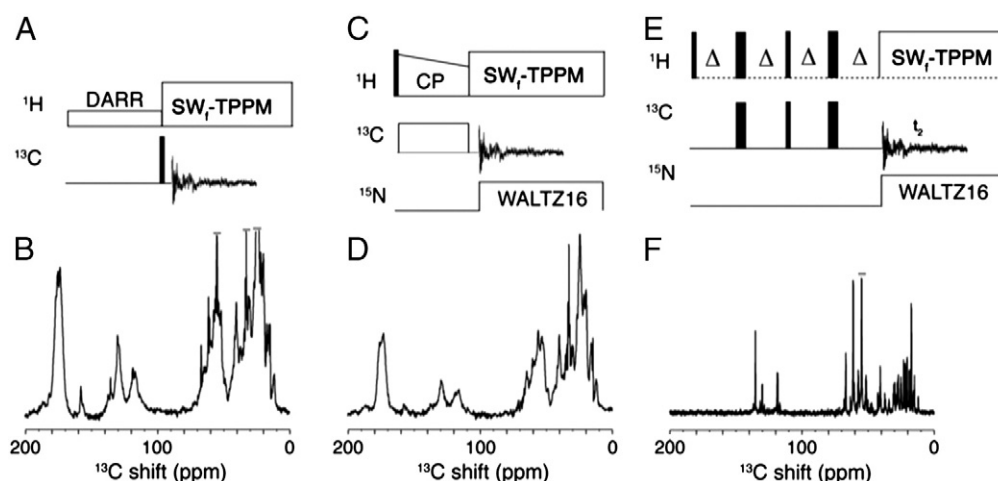

Fig. 8. One-dimensional pulse sequences for ^{1}H to ^{13}C cross polarization (CP) and experimental results obtained from a uniformly ^{13}C and ^{15}N labeled sample of CXCR1 in DMPC phospholipid bilayers. A. and B. Nuclear Overhauser polarization transfer in MAS (NOP-MAS). C. and D. Hartmann–Hahn CP MAS. E. and F. Insensitive nuclei enhanced by polarization transfer (INEPT) MAS. B., D., and F. [1]H decoupled ^{13}C-detected one-dimensional spectra NMR obtained using the pulse schemes shown directly above. Experiments were carried out with 10 kHz MAS at 30 °C. Continuous wave radio frequency irradiation with amplitude less than 10 kHz was applied for 1 s for NOP-MAS. 100 kHz RF with swept frequency two-pulse phase modulation (SW$_f$-TPPM) was applied for ^{1}H decoupling. 62 kHz RF irradiation was applied on the ^{13}C nuclei in all experiments. Cross-polarization transfer in CP-MAS was obtained with 1 ms mixing and for t periods in INEPT. One-dimensional data from CP and NOP were recorded with 100 scans each and 1000 scans for INEPT.
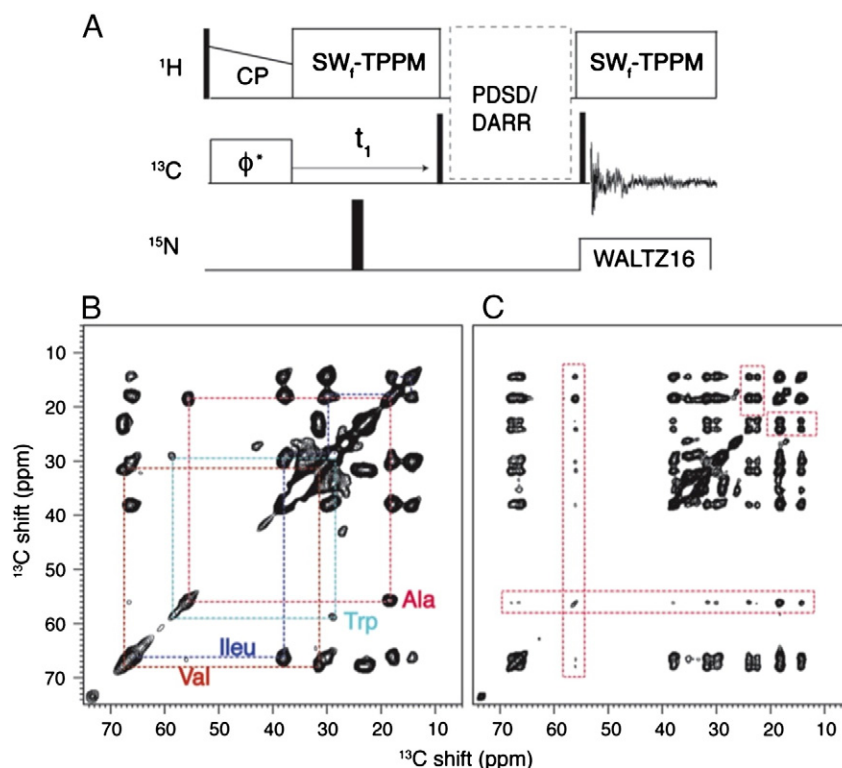
Fig. 9. $^{13}C/^{13}C$ homonuclear correlation spectra of the trans-membrane domain of Vpu in DMPC bilayers obtained at 15 °C. The sample consisted of 2 mg of labeled protein in 10 mg DMPC. A. Pulse scheme to record spin-exchange data. Thin and thick solid lines represent 90° and 180° pulses, respectively. B. and C. Two-dimensional NMR spectra correlating aliphatic carbons obtained for 50 ms and 500 ms PDSD mixing with 11 kHz MAS, respectively. The dashed lines in B. correlate ^{13}C shifts within a residue type. The rectangular boxes in C. represent the cross peaks that resulted from long mixing. They are potentially from inter-residue or inter-helical contacts between residues. (ϕ^*) represents the phase sensitive data acquisition using States mode. The spectra were obtained from 5 ms and 15 ms chemical shift evolution in indirect and direct acquisition dimensions, respectively.

and inter-helix contacts through signals from side chain carbons. Additionally, the variations in cross peaks intensities can provide semi-quantitative distance measurements. Thus in addition to having a primary role in the resonance assignment process, homonuclear

spin-exchange provides valuable information about distances that contribute to the protein structure calculations.

Both two-dimensional homonuclear correlation, as in Fig. 9, and heteronuclear correlation, as in Fig. 10, spectra provide enough signals
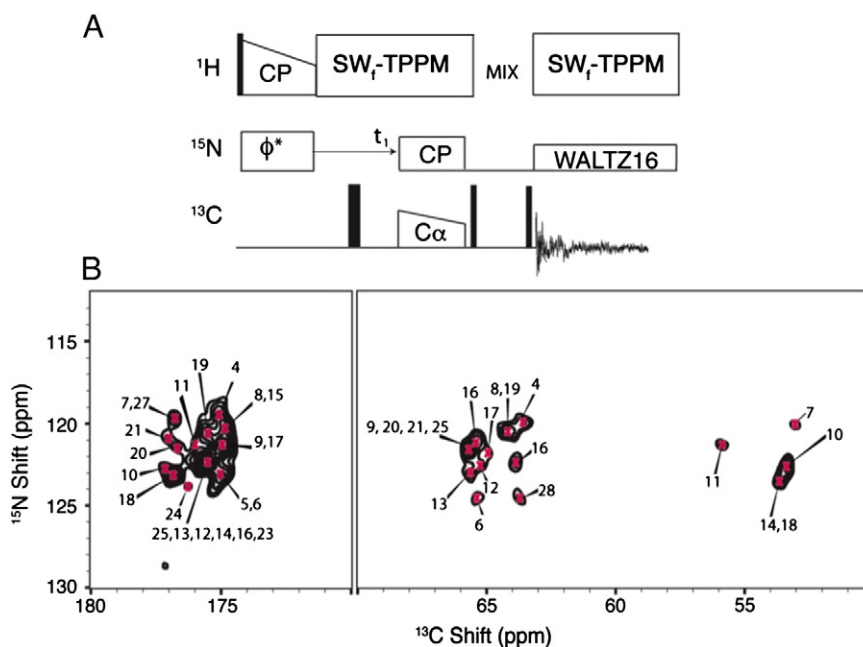

Fig. 10. Two-dimensional $^{15}N/^{13}C$ shift correlation spectrum obtained from a uniformly ^{13}C and ^{15}N labeled sample of the trans-membrane domain of Vpu in DMPC bilayers at 15 °C. A. Pulse sequence used to obtain the two-dimensional data. B. N(CA)CX two-dimensional spectrum correlating the ^{13}C and ^{15}N nuclei within a residue. (ϕ^*) represents the phase sensitive data acquisition under States mode. ^{1}H was decoupled with 100 kHz RF during isotropic chemical shift evolution and DCP [48].

with two characteristic frequencies to give unique resonance patterns that serve as "fingerprints" of the folded protein. The correlation between ^{13}C and ^{15}N nuclei provides not only a high-resolution spectrum, but also the measurement of both ^{15}N and ^{13}C chemical shift frequency measurements, which are complementary to those observed in the homonuclear correlation spectra. The pulse sequence diagrammed in Fig. 10A establishes $^{13}C/^{15}N$ heteronuclear correlation with ^{13}C detection. The ^{15}N magnetization resulting from CP undergoes isotropic chemical shift evolution under heteronuclear decoupling, provided by a single 180° ^{13}C pulse as in Fig. 10A. After the chemical shift evolution during t1, the ^{15}N magnetization is transferred selectively to either ^{13}CA or ^{13}CO. It is possible to invoke direct ^{13}C detection at this point to obtain a two-dimensional heteronuclear correlation spectrum of directly bonded ^{13}C and ^{15}N nuclei. However, the pulse sequence in Fig. 10A is more elaborate, since the ^{13}C magnetization is subsequently transferred to other ^{13}C sites using a short spin-exchange mixing period followed by the direct ^{13}C detection under heteronuclear decoupling. The N(CA)CX heteronuclear correlation spectrum of the transmembrane domain of Vpu is shown in Fig. 10B. Each cross peak in the spectrum provides chemical shift information for ^{13}CO, ^{13}CA, and ^{15}N nuclei in a single residue. The residue numbers are assigned to each cross peak following sequential assignment experiments.

Depending upon the correlation time and line widths of the protein resonances, magnetization is transferred using through-bond J-couplings or through-space dipolar couplings. J-based spectroscopic techniques can be used in MAS solid state NMR because the combination of fast MAS and radio frequency irradiations provide high-resolution spectra comparable to those obtained by solution NMR methods applied to soluble proteins. However, due to dipolar truncation under MAS, polarization transfers using through-space methods can be limited to one-bond transfers, which facilitate sequential assignments through unidirectional coherence transfer pathways along the backbone.

Sequential assignment of resonances typically begins with the two basic two-dimensional correlation experiments shown in Figs. 9 and 10, $^{13}C/^{13}C$ homo-nuclear spin exchange and coherence transfer between ^{15}N and ^{13}C, respectively. These two-dimensional experiments are the basic building blocks for the higher dimensional experiments required for resolution and assignment of protein spectra. The triple-resonance experiments NCACO, NCOCA, and CANCO, diagrammed in Fig. 11A, C, and E, respectively, utilize unidirectional coherence transfer pathways between ^{15}N and ^{13}C nuclei along the peptide backbone [120]. In NCACO and NCOCA class experiments, both hetero-nuclear polarization transfer and homo-nuclear spin exchange techniques are utilized. In contrast, in CANCO, ^{15}N and ^{13}CA chemical shifts evolve both before and after ^{15}N to ^{13}CA double cross polarization (DCP). $^{13}CA/^{13}CO$ correlation is established with a short mixing interval; as a result, ^{15}N and ^{13}C isotropic chemical shifts are correlated in three-dimensions. The NCOCA experiment follows the same coherence transfer pathways as NCACO except that DCP is used to transfer magnetization from ^{15}N to ^{13}CO of the preceding residue. Using both NCACO and NCOCA data, correlations between signals in adjacent residues can be established. CA and CO chemical shifts are correlated to the ^{15}N shifts within the residue as well as the adjacent one. This provides an efficient means for identifying amide pairs in neighboring residues, a key step in making sequential resonance assignments.

The well-dispersed chemical shifts of side chain resonances can also be utilized in the assignment process with NCACB, NCACX, and NCOCX experiments. Additionally, when three-dimensional NCACX data are available, side chain resonance patterns can often be observed in the direct ^{13}C dimension, enabling residue types to be identified through the statistical evaluation of their chemical shift frequencies. The disadvantage of this method is that the presence of long-range correlations to inter-residue side chain nuclei can lead to complicated spectra. Similarly, unidirectional cross-polarization transfer techniques are used in CANCO class experiments where inter- and intra- residue ^{13}C

correlations are established in three steps. The experiment starts with polarization transfer from ^{1}H to ^{13}C followed by a ^{13}CA chemical shift evolution under ^{1}H and ^{15}N decoupling. The magnetization from ^{13}CA is then transferred to ^{15}N, followed by the ^{15}N chemical shift evolution under ^{1}H and ^{13}C decoupling. In the last step, the ^{15}N magnetization is transferred to ^{13}CO of the preceding residue. The three-dimensional data correlates ^{13}CA and ^{15}N shifts within a residue to those of the ^{13}CO from the preceding residue. The assignment techniques briefly described here have been successfully applied to uniformly ^{13}C and ^{15}N labeled membrane proteins with between one and seven trans-membrane helices.

Experimental results obtained on a 41 kDa (7 trans-membrane helices) G-protein coupled receptor are shown in Fig. 11. The results were obtained from a uniformly ^{13}C and ^{15}N labeled sample of CXCR1 in DMPC liposomes utilizing the pulse sequences diagrammed in Fig. 11A, C, and E. The two-dimensional planes correlating CA and CO shifts were obtained at the ^{15}N chemical shift frequency of 120.1 ppm for NCACO (Fig. 11B), NCOCA (Fig. 11D) and CANCO (Fig. 11F). Each cross peak in Fig. 11B and F represents single site resolution for carbon nuclei in a single residue type. The ^{13}C frequencies correlated in Fig. 11B and F are aligned for ^{15}N shifts from adjacent residues. In Fig. 11G, inter residue CA and CO shifts are correlated and facilitate the assignment of backbone resonances. The assignments of the cross-peaks in Fig. 11B are denoted by the residue numbers. Representative strip plots for sequential assignments in the backbone are illustrated for ten contiguous residues in Fig. 11G with NCACO and NCOCA data.

3.1. Structural restraints

As illustrated in Figs. 1 and 2, motionally averaged anisotropic heteronuclear dipole-dipole and chemical shift interactions provide angular restraints. In RA solid-state NMR, the frequency of the parallel edge of the motionally averaged powder pattern for a particular site provides an angular measurement relative to a defined axis; in the case of membrane proteins it is the bilayer normal. Because the motionally averaged ^{1}H–^{13}C, ^{1}H–^{15}N dipolar coupling (DC) and ^{13}C, ^{15}N chemical shift (CS) powder patterns are axially symmetric, the frequency of the parallel discontinuity can also be obtained by measuring the perpendicular discontinuity or the span of the powder pattern with. The experimental methods used in the recoupling and measurement of motionally averaged ^{1}H–^{13}C heteronuclear dipolar coupling powder patterns are shown in Fig. 12B and C.

The pulse sequences diagrammed in Fig. 12A and D use decoupling and recoupling techniques to correlate the dipolar couplings with isotropic chemical shifts. In MAS solid-state NMR heteronuclear dipolar interactions are recoupled using pulse schemes based on Hartmann–Hahn match condition and its variants [121,122]. Symmetry-based pulse sequences [123,124] provide a high degree of flexibility in the application of experimental methods. Heteronuclear dipolar recoupling using symmetry based radio frequency pulses applied on a single channel can restore the effect on the other nuclei and are measured with direct detection of ^{13}C or ^{15}N nuclei. In particular, ^{15}N edited ^{13}C detection pulse schemes are integral to many high-resolution multidimensional experiments. Experimental protocols are now well optimized to measure ^{1}H–^{15}N and ^{1}H–^{13}C heteronuclear dipolar frequencies from membrane proteins in phospholipid bilayers.

Heteronuclear dipolar couplings are recoupled under MAS in two ways, either by proton evolved local field (PELF) or by separated local field (SLF) spectroscopy using symmetry based pulses. $R18^{7}_{1}$ and $R18^{5}_{2}$ pulse schemes are particularly useful at moderate spinning rates [123]. Several other pulse sequences based on symmetry principles with rotor synchronization are useful for fast and ultra fast spinning [125]. $R18^{7}_{1}$ consists of a pair of $180_{70}180_{-70}$ pulses where each $180°$ pulse occupies exactly 1/18 of a rotor period. The two-pulse phase modulation with alternating phase shift of $70°$ in $R18^{7}_{1}$ cycle efficiently recouples the dipolar frequencies under 11 kHz spinning. However,
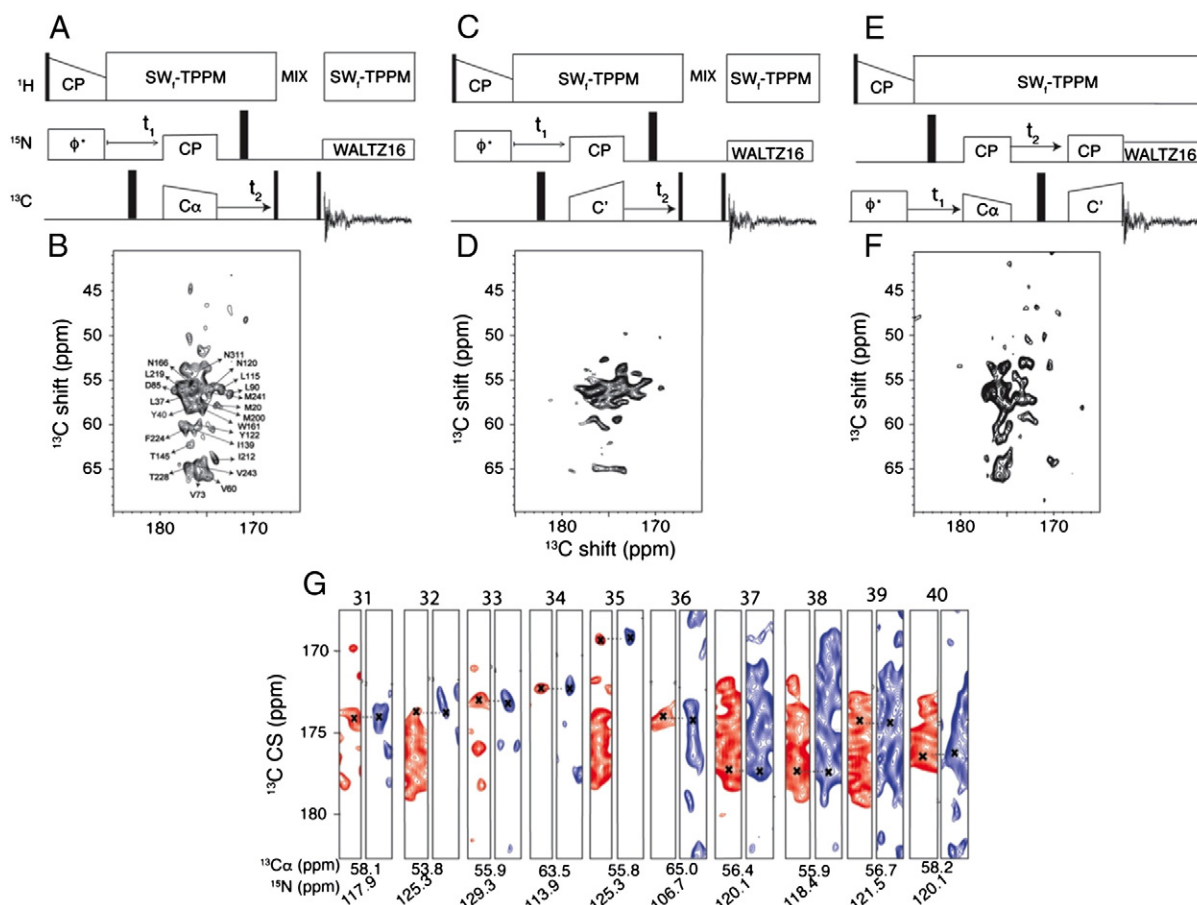
Fig. 11. Pulse sequences and spectra relevant to the three-dimensional correlation spectroscopy used to make sequential resonance assignments. A. and B. NCACO. C. and D. NCOCA. E. and F. CANCO. Thin and wide solid lines represent the 90° and 180° pulses, respectively. B., D. and F. are ^{13}CA/^{13}CO two-dimensional planes obtained at 120.1 ppm ^{15}N chemical shift. The three-dimensional data were collected from a uniformly ^{13}C and ^{15}N labeled sample of CXCR1 in DMPC bilayers at 30 °C. G. Strip plot for residues 31–40 with nitrogen and carbon chemical shifts given below. Assigned residues are marked in the two-dimensional plane (D) obtained from NCACO three-dimensional data. Data were collected with 4–5 ms ^{13}C and 6 ms ^{15}N isotropic shift evolution in indirect dimensions, and 12 ms during direct ^{13}C acquisition under heteronuclear decoupling. Equal numbers of data points in the indirect dimension were linear predicted. 0.2 ppm line broadening was used in the direct dimension during data processing. Each of the three-dimensional data sets was collected with approximately 1000 scans.
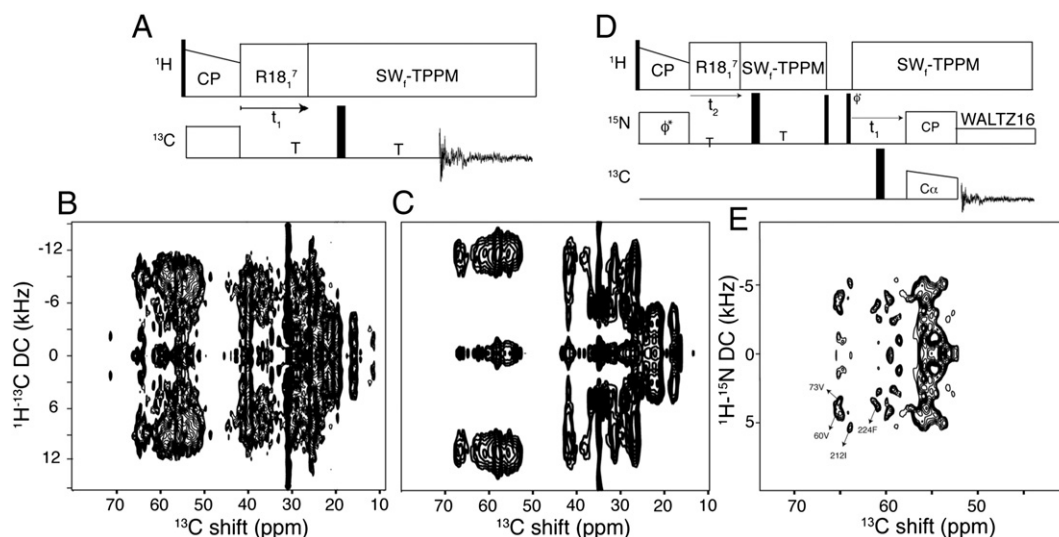

Fig. 12. Two- and three-dimensional separated local field (SLF) NMR spectra obtained from a uniformly ^{13}C and ^{15}N labeled sample of CXCR1 in DMPC bilayers. A. Pulse scheme used for recording the two-dimensional SLF data. B. ^{1}H-^{13}C DC/^{13}C CS two-dimensional SLF correlation obtained at 30 °C. C. Same as B except at 10 °C. D. Pulse sequence for three-dimensional SLF NMR with ^{15}N editing and ^{13}C detection. Thin and wide solid lines represent the 90° and 180° pulses, respectively. (φ*) represents the phase sensitive data acquisition under States mode. E. Two-dimensional SLF plane from the three-dimensional spectrum correlating ^{13}CA shifts with ^{1}H-^{15}N DC obtained at 120.1 ppm ^{15}N shift. Cross peaks with single site resolution are marked with residue numbers.

R18$_1^7$ irradiation leads to recoupling of ^{1}H–^{13}C dipolar couplings and ^{1}H chemical shift anisotropies when applied on the ^{1}H channel whereas homo-nuclear dipolar interactions among the ^{1}H spins are suppressed. The two-dimensional ^{13}C detected SLF experiment correlating ^{1}H–^{13}C DC frequencies with ^{13}C isotropic chemical shifts is diagrammed in Fig. 12. The recoupling in the two-dimensional experiment was carried out in a constant time spin echo period followed by direct ^{13}C detection. Spectra were obtained at temperatures above and below the gel to liquid crystalline phase transition of the phospholipids. Due to the variation in ^{1}H–^{13}C bond angles apparent in the presence of fast rotational diffusion, there is a wide spread of DC frequencies of the ^{13}CA resonances in the spectrum in Fig. 12A. In contrast, at a temperature below the phase transition where the protein is not undergoing rotational diffusion compared to the span of the DC powder pattern, all of the ^{13}CA resonances (40 ppm–70 ppm) have the full static value for the dipolar couplings. The two-dimensional data in Fig. 12 illustrate the general features of the spectroscopic phenomenon being investigated. As shown with the spectral plane in Fig. 12E, higher dimensional experiments are required to obtain single-site resolution in relatively large membrane proteins for the measurements that provide the angular restraints for the structure calculations.

Fig. 13 compares the static ^{1}H–^{13}C dipolar powder pattern (top) to two different motionally averaged dipolar powder patterns, which were derived from the experimental data shown below each powder pattern in the figure. The powder pattern with parallel edge frequencies of 28.8 kHz is from a ^{1}H–^{13}C bond positioned with an angle of 152° from the bilayer normal. The much smaller coupling of 7.2 kHz is associated with a bond at 48°, near the "magic angle", which would have given a dipolar coupling of 0 kHz. The magnitudes of the frequency spread between the parallel edges of the powder patterns directly translate to structural restraints shown on the left of Fig. 13. Importantly, all angles are measured relative to the same external axis, in this case the bilayer normal, so that errors do not accumulate along the backbone. This is a critical feature for the success of the method.

4. Structure calculations

The advantage of using DCs and CSAs measured from solid state NMR is that they are straightforward to interpret since their order tensors are known *a priori*. They can be measured directly from the single line resonances of OS solid-state NMR spectra or by employing the recoupling techniques in MAS solid-state NMR described above. The MAS approach has the important advantage that multiple peaks can

be resolved and assigned through the use of triple resonance ^{1}H/^{13}C/^{15}N MAS experiments in uniformly labeled samples, and the isotropic chemical shifts provide dihedral angle restraints. While dihedral angle and distance restraints serve as internal references, orientation restraints are referenced to an external frame (*e.g.*, the bilayer normal). This is illustrated in Fig. 13 for ^{1}H–^{13}CA dipolar couplings where the angles relative to the bilayer normal are shown. They are ultimately used as orientational restraints in the calculations of the protein structure.

Rosetta is one of the most successful programs for *de novo* structure prediction from amino acid sequence for both soluble [126–128] and membrane proteins [129,130]. It effectively combines multiple fragment replacement (MFR) [131] with Monte Carlo simulated annealing, to generate structures from polypeptide fragments selected on the basis of homology modeling and search of the Protein Data Base (PDB). Rosetta prediction involves three stages. First, overlapping polypeptide fragments (typically 3- and 9-residue long) are generated based on homology to the protein's amino acid sequence. Second, a low-resolution structure is generated by a Monte Carlo MFR procedure, where the backbone heavy atoms and side chain centroids are considered explicitly while minimizing a coarse-grained empirical energy term that includes van der Waals packing, hydrogen bonding and desolvation terms. Finally, the structure is refined using Monte Carlo and gradient-based minimization of all torsional degrees of freedom in a physically realistic, empirical, all-atom force field. Rosetta prediction accuracy is limited to proteins with <150 amino acids primarily because native structures are seldom sampled in unbiased trajectories, even though they usually have lower energies than non-native conformations. This problem is alleviated by guiding fragment selection and assembly with isotropic CS [132,133] and DCs [134–136].

CS-Rosetta utilizes database values of isotropic CS [137,138]; the implementation of orientation restraints enables direct model refinement of the models against the NMR data. Furthermore, prior knowledge of the solid-state NMR alignment tensors facilitates fragment selection and assembly compared to solution NMR residual DCs [136]. Fragments of varying lengths are generated from the input data in Rosetta and each fragment is aligned in the frame of the membrane using the experimental DCs and rigid body MD in Xplor-NIH. Solid-state NMR DCs are extremely useful for guiding fragment selection and assembly, since their values incorporate full knowledge of the sample's alignment tensor and thus directly reflect molecular orientation in the membrane. Each aligned fragment is scored using the equation and parameters outlined and the best scoring fragments are accepted. The DC-filtered fragments are further used to assemble coarse-grained Rosetta models, which are then refined in the Rosetta all-atom force field and scored by Rosetta all-atom energy and DC RMSD. Analogous to CS-Rosetta [133], convergence of the structure generation process are based on how well the coordinates of the lowest energy structures agree with one another; by plotting Rosetta all-atom energy as a function of backbone and DC RMSD relative to the model with the lowest energy. For CS-Rosetta, such diagrams identify reliable structures based on RMSD relative to the lowest-energy structure. 10 lowest energy models found to cluster within <2 Å of the lowest energy model are selected for further refinement by restrained MD in Xplor-NIH.

5. Summary

The measurement of angular restraints relative to an external axis provides sufficient input to calculate the three-dimensional structure of a protein. These measurements are well suited for membrane proteins that undergo rapid rotational diffusion in phospholipid bilayers. Also, these measurements are particularly forgiving with respect to experimental errors and uncertainties regarding the principal values and orientations of the tensors in the molecular frame because site-to-site errors do not accumulate. Each measurement is made independently relative to a common external axis, in this case the bilayer normal. In related approaches, the axis can be the direction of
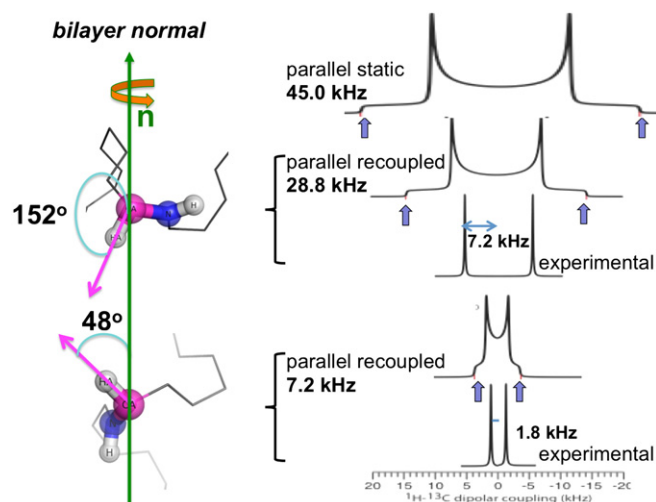

Fig. 13. Angles between HA–CA bond vectors and bilayer normal determined from rotationally averaged ^{1}H–^{13}C Pake doublets.

the magnetic field, orthogonal to the field, or relative to the mechanical alignment on glass plates.

A uniaxially aligned sample, where the direction of the molecular alignment is parallel to that of the magnetic field, is the next most general type of sample after a single crystal. In this case, the sample has one direction of orientation and the other two directions are random or undefined. What is most notable is that static samples are capable of yielding very high-resolution spectra when aligned parallel to the field, the line shapes become broad and complex when they are tilted away from parallel [52]. This is seen most dramatically when the axis of alignment is perpendicular to the direction of the field. A characteristic partial powder pattern is observed in these situations. However, the situation is greatly simplified when the molecule of interest undergoes fast rotational diffusion about a single axis.

Membrane proteins in phospholipid bilayers can be aligned mechanically between glass plates. As with uniaxially aligned polymers, when the axis of alignment is parallel to the field, single line resonances are observed regardless of whether any molecular motion is present. Magnetically aligned samples of membrane proteins were originally sought as direct replacements for mechanically aligned samples, and once it was discovered that the lanthanide ions added to the lipids could "flip" the alignment so that the bilayer normals were parallel to the field [139] then that became feasible. There is considerably more flexibility with magnetically aligned systems because the proteins undergo fast rotational diffusion about the bilayer normal.

OS solid-state NMR is based on the measurement of angular restraints as input for structure calculations in order to determine the structures of proteins. Sample preparation is a key component of experimental design, and often the limiting factor in the selection of protein samples for study. Experimental results on mechanically and magnetically aligned samples are directly compared to those from unoriented samples, demonstrating the equivalence of the angularly dependent frequencies from the chemical shift and dipole–dipole interactions as long as the membrane proteins undergo fast rotational diffusion about the bilayer normal and that this axis is collinear with the axes of alignment defined by the direction of the bilayer normal relative to the magnetic field. This expands the possibilities for applying the basic principles of OS solid-state NMR to unoriented samples, including those with many labeled sites with the use of MAS solid-state NMR methods that reveal or recouple the powder patterns from the motionally averaged chemical shift and dipole–dipole interactions. Angular restraints from these two sources for each peptide plane are sufficient to determine the backbone structure of a protein, and it can be extended to side chains for complete structure determination

of membrane proteins in their native liquid crystalline phospholipid bilayer environment.

Fig. 14 summarizes the current state of structure determination of membrane proteins by RA solid-state NMR. The comparison of the structure of the truncated version of MerF (MerFt) has a distinctly different structure than that of the full-length protein (MerF). The N-terminal residues are mobile and unstructured in micelles, yet when they are removed, a drastic rearrangement of the tertiary structure occurs, as shown in Fig. 15. The structure of p7 in bilayers is shown in Fig. 16, and it too has a distinctly different structure from than that determined in micelles. These examples serve to demonstrate the points originally raised by Anfinsen [32], which are that the structure of a protein is determined by its primary sequence of amino acids, and if that is altered, then the structure of the protein is changed (MerFt vs. MerF), and discussed by Cross [19], which is that the environment has a major impact on the structure with large differences in structure for p7 determined in micelles and in bilayers.

The three-dimensional structure of the 81-residue mercury transporter MerF determined in liquid crystalline phospholipid bilayers under physiological conditions by rotationally aligned solid-state NMR has two long helices, which extend well beyond the bilayer, with a well-defined interhelical loop. Truncation of the N-terminal 12 residues, which are mobile and unstructured when the protein is in micelles, results in a structural rearrangement when the protein is in a bilayer environment [21]. In the full-length protein, the N-terminal helix is aligned nearly parallel to the membrane normal and forms an extension of the first transmembrane helix. By contrast, these same residues adopt a perpendicular orientation as a helix in the truncated protein. Clearly, major changes in protein structure can result from differences in amino acid sequence (e.g., full-length vs. truncated proteins) as well as the use of a non-native membrane mimetic environment (e.g., micelles) vs. liquid crystalline phospholipid bilayers.

The superposition of the structures of the full-length (aqua) and truncated (magenta) MerF proteins in Fig. 15 is highly informative. Both structures were determined under identical sample conditions and methods; therefore, the observed structural rearrangement results solely from the alteration of the amino acid sequence of the protein. In contrast to the N-terminal truncation, the C-terminal truncation does not result in significant structural changes. This comparison provides strong evidence of the importance of studying unmodified membrane proteins.

Hepatitis C virus (HCV) protein p7 plays an important role in the assembly and release of mature virus particles. This small 63-residue membrane protein has been shown to have channel activity, which
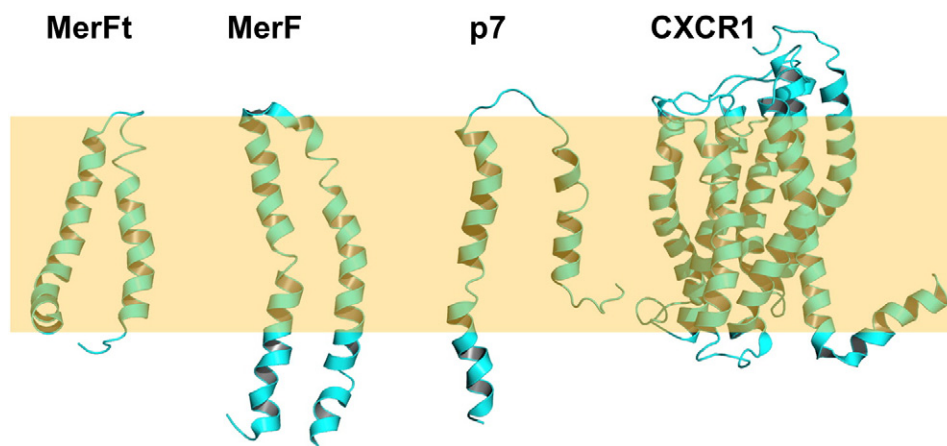

Fig. 14. Structures of membrane proteins determined in phospholipid bilayers by RA solid-state NMR. From left to right: the truncated form of the mercury transport membrane protein MerFt [24] (PDB code: 2LJ2), the full-length mercury transport membrane protein MerF [21] (PDB code: 2M67), the viral membrane protein p7 from the human hepatitis C virus, and the 350-residue chemokine receptor CXCR1 [25] (PDB code: 2LNL).
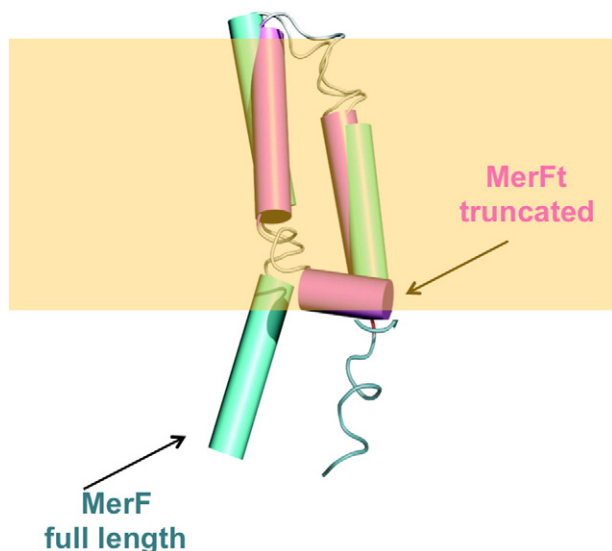
Fig. 15. Comparison of the structures of truncated 60-residue MerFt (magenta) and full-length 81-residue MerF (aqua) showing the structural distortions resulting from truncation of residues that are mobile and unstructured in micelles [21].

may contribute to its biological functions. The structure of this protein has been determined in three different membrane environments, two different types of micelles, and phospholipid bilayers. The structure that we determined in DHPC micelles (Fig. 16A) and DMPC bilayers (Fig. 16B) are compared in schematic backgrounds of the lipids in their respective assemblies. The protein structures differ widely from each other. Because the phospholipid bilayers provide a near-native environment, we can place some confidence on the structure determined by rotationally aligned solid-state NMR. The dramatic variation in structures in Fig. 16 demonstrates how important it is to characterize membrane proteins in phospholipid bilayers rather than micelles.

Now that we have the ability to determine the structures of membrane proteins in liquid crystalline phospholipid bilayers under physiological conditions, it will be possible to exploit comparative studies of apo-proteins as well as their complexes with small and large molecular species. It will also be possible to characterize the influence of the amino acid sequence on the tertiary structure of the proteins and the effects of the phospholipid bilayer on their structures.
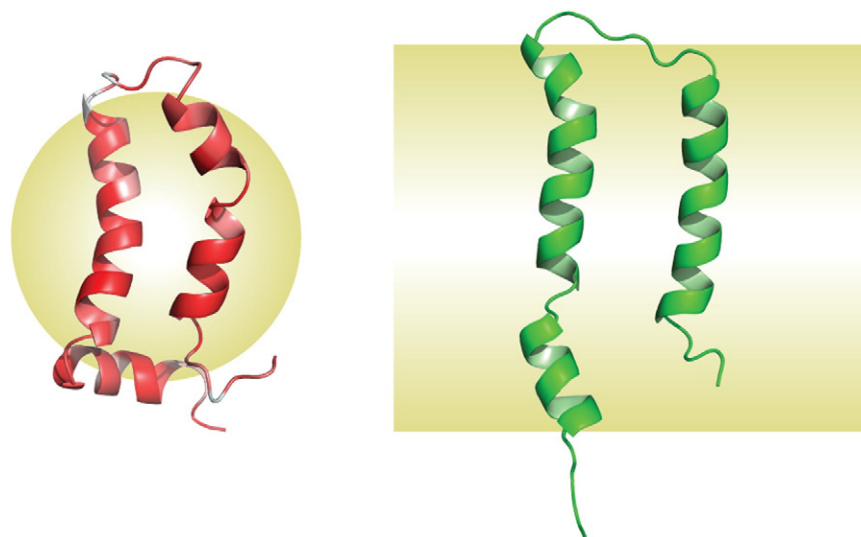
References

[1] J.C. Kendrew, G. Bodo, H.M. Dintzis, R.G. Parrish, H.W. Wyckoff, D.C. Philips, A three-dimensional model of the myoglobin molecule obtained by X-ray analysis, Nature 181 (1958) 666.

[2] M.F. Perutz, M.G. Rossman, A.F. Cullis, H. Muirhead, W. Georg, Structure of hemoglobin: a three-dimensional Fourier synthesis at 5.5 A resolution, obtained by X-ray analysis, Nature 185 (1960) 416–422.

[3] A.D. Kline, W. Braun, K. Wuthrich, Determination of the complete three-dimensional structure of the a-amylase inhibitor Tendamistat in aqueous solution by nuclear magnetic resonance and distance geometry, J. Mol. Biol. 204 (1988) 675–724.

[4] F. Castellani, B. van Rossum, A. Diehl, M. Schubert, K. Rehbein, H. Oschkinat, Structure of a protein determined by solid-state magic-angle-spinning NMR spectroscopy, Nature 420 (2002) 98–102.

[5] S.J. Opella, M.H. Frey, T.A. Cross, Detection of individual carbon resonances in solid proteins, J. Am. Chem. Soc. 101 (1979) 5856–5857.

[6] T.A. Cross, S.J. Opella, Protein structure by solid state NMR, J. Am. Chem. Soc. 105 (1983) 306–308.

[7] S. Yan, C.L. Suiter, G. Hou, H. Zhang, T. Polenova, Probing structure and dynamics of protein assemblies by magic angle spinning NMR spectroscopy, Acc. Chem. Res. 46 (2013) 2047–2058.

[8] A. Loquet, B. Habenstein, A. Lange, Structural investigations of molecular machines by solid-state NMR, Acc. Chem. Res. 46 (2013) 2070–2079.

[9] M. Weingarth, M. Baldus, Solid-state NMR-based approaches for supramolecular structure elucidation, Acc. Chem. Res. 46 (2013) 2037–2046.

[10] A.C. Zeri, M.F. Mesleh, A.A. Nevzorov, S.J. Opella, Structure of the coat protein in fd filamentous bacteriophage particles determined by solid-state NMR spectroscopy, Proc. Natl. Acad. Sci. U. S. A. 100 (2003) 6458–6463.

[11] R. Tycko, Solid-state NMR studies of amyloid fibril structure, Annu. Rev. Phys. Chem. 62 (2011) 279–299.

[12] R.R. Ketchem, W. Hu, T.A. Cross, High-resolution conformation of gramicidin A in a lipid bilayer by solid-state NMR, Science 261 (1993) 1457–1460.

[13] F.M. Marassi, S.J. Opella, Simultaneous assignment and structure determination of a membrane protein from NMR orientational restraints, Protein Sci. 12 (2003) 403–411.

[14] T.A. Cross, J.A. DiVerdi, S.J. Opella, Strategy for nitrogen NMR of biopolymers, J. Am. Chem. Soc. 104 (1982) 1759–1761.

[15] A.E. McDermott, Structural and dynamic studies of proteins by solid-state NMR spectroscopy: rapid movement forward, Curr. Opin. Struct. Biol. 14 (2004) 554–561.

[16] B.J. Wylie, L.J. Sperling, A.J. Niewuwkoop, W.T. Franks, E. Oldfield, C.M. Rienstra, Ultrahigh resolution protein structures using NMR chemical shift tensors, Proc. Natl. Acad. Sci. 108 (2011) 16974–16979.

Fig. 16. Comparison of the structures of full-length 63-residue p7 in micelles and bilayers. A. Structure in DHPC micelles. B. Structure in DMPC bilayers. The structure in micelles is drastically distorted from that in bilayers. The cartoon micelle suggests that the distortion is caused by the requirement of the N-terminal helix to be in a hydrophobic environment.

[17] S.J. Opella, Structure determination of membrane proteins by nuclear magnetic resonance spectroscopy, Annu. Rev. Anal. Chem. 6 (2013) 305–328.

[18] D.T. Murray, N. Das, T.A. Cross, Solid state NMR strategy for characterizing native membrane protein structures, Acc. Chem. Res. 46 (2013) 2172–2181.

[19] H.X. Zhou, T.A. Cross, Influences of membrane mimetic environments on membrane protein structures, Annu. Rev. Biophys. 42 (2013) 361–392.

[20] T.A. Cross, D.T. Murray, A. Watts, Helical membrane protein conformations and their environment, Eur. Biophys. J. 42 (2013) 731–755.

[21] G.J. Lu, Y. Tian, N. Vora, F.M. Marassi, S.J. Opella, The structure of the mercury transporter MerF in phospholipid bilayers: a large conformational rearrangement results from N-terminal truncation, J. Am. Chem. Soc. 135 (2013) 9299–9302.

[22] S.J. Opella, F.M. Marassi, J.J. Gesell, A.P. Valente, Y. Kim, M. Oblatt-Montal, M. Montal, Structures of the M2 channel-lining segments from nicotinic acetylcholine and NMDA receptors by NMR spectroscopy, Nat. Struct. Biol. 6 (1999) 374–379.

[23] S.H. Park, A.A. Mrse, A.A. Nevzorov, M.F. Mesleh, M. Oblatt-Montal, M. Montal, S.J. Opella, Three-dimensional structure of the channel-forming trans-membrane domain of virus protein "u" (Vpu) from HIV-1, J. Mol. Biol. 333 (2003) 409–424.

[24] B.B. Das, H.J. Nothnagel, G.J. Lu, W.S. Son, Y. Tian, F.M. Marassi, S.J. Opella, Structure determination of a membrane protein in proteoliposomes, J. Am. Chem. Soc. 134 (2012) 2047–2056.

[25] S.H. Park, B.B. Das, F. Casagrande, Y. Tian, H.J. Nothnagel, M. Chu, H. Kiefer, K. Maier, A.A. De Angelis, F.M. Marassi, S.J. Opella, Structure of the chemokine receptor CXCR1 in phospholipid bilayers, Nature 7426 (2012) 779–783.

[26] T.A. Cross, H. Dong, M. Sharma, D.D. Busath, H.X. Zhou, M2 protein from influenza A: from multiple structures to biophysical and functional insights, Curr. Opin. Virol. 2 (2012) 128–133.

[27] M. Gerstein, A structural census of genomes: comparing bacterial, eukaryotic, and archaeal genomes in terms of protein structure, J. Mol. Biol. 274 (1997) 562–576.

[28] F.M. Marassi, B.B. Das, G.J. Lu, H.J. Nothnagel, S.H. Park, W.S. Son, Y. Tian, S.J. Opella, Structure determination of membrane proteins in five easy pieces, Methods 55 (2011) 363–369.

[29] M. Edidin, Rotational and translational diffusion in membranes, Annu. Rev. Biophys. Bioeng. 3 (1974) 179–201.

[30] R.J. Cherry, U. Muller, G. Schneider, Rotational diffusion of bacteriorhodopsin in lipid membranes, FEBS Lett. 80 (1977) 465–469.

[31] S. Park, B.B. Das, A.A. DeAngelis, M. Scrima, S.J. Opella, Mechanically, magnetically, and 'rotationally aligned' membrane proteins in phospholipid bilayers give equivalent angular constraints for NMR structure determination, J. Phys. Chem. B 114 (2010) (13995–13003).

[32] C.B. Anfinsen, Principles that govern the folding of protein chains, Science 181 (1973) 223–230.

[33] M. Tang, G. Comellas, C.M. Rienstra, Advanced solid-state NMR approaches for structure determination of membrane proteins and amyloid fibrils, Acc. Chem. Res. 46 (2013) 2080–2088.

[34] M. Sharma, M. Yi, H. Dong, H. Qin, E. Peterson, D.D. Busath, H.X. Zhou, T.A. Cross, Insight into the mechanism of the influenza A proton channel from a structure in a lipid bilayer, Science 330 (2010) 509–512.

[35] O.C. Andronesi, S. Becker, K. Seidel, H. Heise, H.S. Young, M. Baldus, Determination of membrane protein structure and dynamics by magic-angle-spinning solid-state NMR spectroscopy, J. Am. Chem. Soc. 127 (2005) 12965–12974.

[36] A.A. De Angelis, S.C. Howell, A.A. Nevzorov, S.J. Opella, Structure determination of a membrane protein with two trans-membrane helices in aligned phospholipid bicelles by solid-state NMR spectroscopy, J. Am. Chem. Soc. 128 (2006) 12256–12267.

[37] B.A. Buck-Koehntop, A. Mascioni, J.J. Buffy, G. Veglia, Structure, dynamics, and membrane topology of stannin: a mediator of neuronal cell apoptosis induced by trimethyltin chloride, J. Mol. Biol. 354 (2005).

[38] R. Verardi, L. Shi, N.J. Traaseth, N. Walsh, G. Veglia, Structural topology of phospholamban pentamer in lipid bilayers by a hybrid solution and solid-state NMR method, Proc. Natl. Acad. Sci. U. S. A. 108 (2011) 9101–9106.

[39] S.H. Park, F.M. Marassi, D. Black, S.J. Opella, Structure and dynamics of the membrane-bound form of Pf1 coat protein: implications of structural rearrangement for virus assembly, Biophys. J. 99 (2010) 1465–1474.

[40] S. Ahuja, N. Jahr, S.C. Im, S. Vivekanandan, N. Popovych, S.V. Le Clair, R. Huang, R. Soong, J. Xu, K. Yamamoto, R.P. Nanga, A. Bridges, L. Waskell, A. Ramamoorthy, A model of the membrane-bound cytochrome b5-cytochrome P450 complex from NMR and mutagenesis data, J. Biol. Chem. 288 (2013) 22080–22095.

[41] R.A. Kinsey, A. Kintanar, E. Oldfield, Dynamics of amino acid side chains in membrane proteins by high field solid state deuterium nuclear magnetic resonance spectroscopy. Phenylalanine, tyrosine, and tryptophan, J. Biol. Chem. 256 (1981) 9028–9036.

[42] C.M. Gall, T.A. Cross, J.A. DiVerdi, S.J. Opella, Protein dynamics by solid-state NMR: aromatic rings of the coat protein in fd bacteriophage, Proc. Natl. Acad. Sci. U. S. A. 79 (1982) 101–105.

[43] B.A. Lewis, G.S. Harbison, J. Herzfeld, R.G. Griffin, NMR structural analysis of a membrane protein: bacteriorhodopsin peptide backbone orientation and motion, Biochemistry 24 (1985) 4671–4679.

[44] S.J. Opella, Structure determination of membrane proteins in their native phospholipid bilayer environment by rotationally aligned solid-state NMR spectroscopy, Acc. Chem. Res. 46 (2013) 2145–2153.

[45] R.A. Cone, Rotational diffusion of rhodopsin in the visual receptor membrane, Nat. New Biol. 236 (1972) 39–43.

[46] R.J. Cherry, Measurement of protein rotational diffusion in membranes by flash photolysis, Methods Enzymol. 54 (1978) 47–61.

[47] S.H. Park, F. Casagrande, B.B. Das, L. Albrecht, M. Chu, S.J. Opella, Local and global dynamics of the G protein-coupled receptor CXCR1, Biochemistry 50 (2011) 2371–2380.

[48] B.B. Das, H. Zhang, S.J. Opella, Dipolar assisted assignment protocol (DAAP) for MAS sold-state NMR of rotationally aligned membrane proteins in phospholipid bilayers, J. Magn. Reson. 242 (2014) 224–232.

[49] H.S. Gutowsky, G.E. Pake, Structural investigations by means of nuclear magnetism. II. Hindered rotation in solids, J. Chem. Phys. 18 (1950) 162–170.

[50] G.E. Pake, Nuclear resonance absorption in hydrated crystals: fine structure of the proton line, J. Chem. Phys. 16 (1948) 327–336.

[51] H.S. Gutowsky, G.B. Kistiakowsky, G.E. Pake, E.M. Purcell, Structural investigations by means of nuclear magnetism. I. Rigid crystal lattices, J. Chem. Phys. 17 (1949) 972–981.

[52] S.J. Opella, J.S. Waugh, Two-dimensional 13C NMR of highly oriented polyethylene, J. Chem. Phys. 66 (1977) 4919–4924.

[53] G.N. Ramachandran, C. Ramakrishnan, V. Sasisekharan, Stereochemistry of polypeptide chain configurations, J. Mol. Biol. 7 (1963) 95–99.

[54] T.A. Cross, S.J. Opella, Protein structure by solid state nuclear magnetic resonance. Residues 40 to 45 of bacteriophage fd coat protein, J. Mol. Biol. 182 (1985) 367–381.

[55] M. Mehring, R.G. Griffin, J.S. Waugh, 19F Shielding tensors from coherently narrowed NMR powder spectra, J. Chem. Phys. 55 (1971) 746–755.

[56] R. Henderson, P.N.T. Unwin, Three-dimensional model of purple membrane obtained by electron microscopy, Nature 257 (1975) 28–32.

[57] H.M. McConnell, W.L. Hubbell, Molecular motion in spin-labeled phospholipids and membranes, J. Am. Chem. Soc. 93 (1971) 314–326.

[58] S.J. Singer, G.L. Nicholson, The fluid mosaic model of the structure of cell membranes, Science 175 (1972) 720–731.

[59] A.C. McLaughlin, P.R. Cullis, M.A. Hemminga, D.I. Hoult, G.K. Radda, G.A. Ritchie, P.J. Seeley, R.E. Richards, Application of 31P NMR to model and biological membrane systems, FEBS Lett. 57 (1975) 213–218.

[60] S.H. Park, A.A. Mrse, A.A. Nevzorov, A.A. De Angelis, S.J. Opella, Rotational diffusion of membrane proteins in aligned phospholipid bilayers by solid-state NMR spectroscopy, J. Magn. Reson. 178 (2005) 162–165.

[61] R. Smith, B.A. Cornell, Dynamics of the intrinsic membrane polypeptide gramicidin A in phospholipid bilayers, Biophys. J. 49 (1986) 117–118.

[62] G.B. Fields, C.G. Fields, J. Petefish, H.E. Van Wart, T.A. Cross, Solid-phase peptide synthesis and solid-state NMR spectroscopy of [Ala3-15N][Val1]gramicidin A, Proc. Natl. Acad. Sci. U. S. A. 85 (1988) 1384–1388.

[63] F. Tian, Z. Song, T.A. Cross, Orientational constraints derived from hydrated powder samples by two-dimensional PISEMA, J. Magn. Reson. 135 (1998) 227–231.

[64] K.-C. Lee, W. Hu, T.A. Cross, 2H NMR determination of the global correlation time of the gramicidin channel in a lipid bilayer, Biophys. J. 65 (1993) 1162–1167.

[65] J.C.C. Chan, R. Tycko, Recoupling of chemical shift anisotropies in solid-state NMR under high-speed magic-angle spinning and in uniformly 13C-labeled systems, J. Chem. Phys. 118 (2003) 8378–8389.

[66] Y.K. Lee, N.D. Kurur, M. Helmle, O.G. Johannessen, N.C. Nielsen, M.H. Levitt, Efficient dipolar recoupling in the NMR of rotating solids. A sevenfold symmetric radiofrequency pulse sequence, Chem. Phys. Lett. 242 (1995) 304–309.

[67] E.P. Vogel, D.P. Weliky, Quantitation of recombinant protein whole cells and cell extracts via solid-state NMR spectroscopy, Biochemistry 52 (2013) 4285–4287.

[68] G.A. Cook, S.J. Opella, Secondary structure, dynamics, and architecture of the p7 membrane protein from hepatitis C virus by NMR spectroscopy, Biochim. Biophys. Acta 1808 (2011) 1448–1453.

[69] S.C. Howell, M.F. Mesleh, S.J. Opella, NMR structure determination of a membrane protein with two transmembrane helices in micelles: MerF of the bacterial mercury detoxification system, Biochemistry 44 (2005) 5196–5206.

[70] J. Hu, H. Qin, F.P. Gao, T.A. Cross, A systematic assessment of mature MBP in membrane protein production: overexpression, membrane targeting and purification, Protein Expr. Purif. 80 (2011) 34–40.

[71] S.H. Park, S. Prytulla, A.A. De Angelis, J.M. Brown, H. Kiefer, S.J. Opella, High-resolution NMR spectroscopy of a GPCR in aligned bicelles, J. Am. Chem. Soc. 128 (2006) 7402–7403.

[72] H. Qin, J. Hu, Y. Hua, S.V. Challa, T.A. Cross, F.P. Gao, Construction of a series of vectors for high throughput cloning and expression screening of membrane proteins from Mycobacterium tuberculosis, BMC Biotechnol. 8 (2008) 51.

[73] K. Thai, J. Choi, C.M. Franzin, F.M. Marassi, Bcl-XL as a fusion protein for the high-level expression of membrane-associated proteins, Protein Sci. 14 (2005) 948–955.

[74] A. Korepanova, J.D. Moore, H.B. Nguyen, Y. Hua, T.A. Cross, F. Gao, Expression of membrane proteins from Mycobacterium tuberculosis in Escherichia coli as fusions with maltose binding protein, Protein Expr. Purif. 53 (2007) 24–30.

[75] J.L. Baneres, A. Martin, P. Hullot, J.P. Girard, J.C. Rossi, J. Parello, Structure-based analysis of GPCR function: conformational adaptation of both agonist and receptor upon leukotriene B4 binding to recombinant BLT1, J. Mol. Biol. 329 (2003) 801–814.

[76] R. Grisshammer, P. Averbeck, A.K. Sohal, Improved purification of a rat neurotensin receptor expressed in Escherichia coli, Biochem. Soc. Trans. 27 (1999) 899–903.

[77] H. Kiefer, J. Krieger, J.D. Olszewski, G. Von Heijne, G.D. Prestwich, H. Breer, Expression of an olfactory receptor in Escherichia coli: purification, reconstitution, and ligand binding, Biochemistry 35 (1996) 16077–16084.

[78] H. Kiefer, K. Maier, R. Vogel, Refolding of G-protein-coupled receptors from inclusion bodies produced in Escherichia coli, Biochem. Soc. Trans. 27 (1999) 908–912.

[79] S.H. Park, F. Casagrande, L. Cho, L. Albrecht, S.J. Opella, Interactions of interleukin-8 with the human chemokine receptor CXCR1 in phospholipid bilayers by NMR spectroscopy, J. Mol. Biol. 414 (2011) 194–203.

[80] N. Sinha, C.V. Grant, S.H. Park, J.M. Brown, S.J. Opella, Triple resonance experiments for aligned sample solid-state NMR of (13)C and (15)N labeled proteins, J. Magn. Reson. 186 (2007) 51–64.

[81] N. Sinha, F.V. Filipp, L Jairam, S.H. Park, J. Bradley, S.J. Opella, Tailoring 13C labeling for triple-resonance solid-state NMR experiments on aligned samples of proteins, Magn. Reson. Chem. 45 (Suppl. 1) (2007) S107–S115.

[82] A. Goldbourt, L.A. Day, A.E. McDermott, Assignment of congested NMR spectra: carbonyl backbone enrichment via the Entner–Doudoroff pathway, J. Magn. Reson. 189 (2007) 157–165.

[83] S.H. Park, C. Yang, S.J. Opella, L.J. Mueller, Resolution and measurement of heteronuclear dipolar couplings of a noncrystalline protein immobilized in a biological supramolecular assembly by proton-detected MAS solid-state NMR spectroscopy, J. Magn. Reson. 237 (2013) 164–168.

[84] C.H. Wu, B.B. Das, S.J. Opella, (1)H-(13)C hetero-nuclear dipole–dipole couplings of methyl groups in stationary and magic angle spinning solid-state NMR experiments of peptides and proteins, J. Magn. Reson. 202 (2010) 127–134.

[85] K. Dornmair, H. Kiefer, F. Jahnig, Refolding of an integral membrane protein. OmpA of Escherichia coli, J. Biol. Chem. 265 (1990) 18907–18911.

[86] H. Kiefer, In vitro folding of alpha-helical membrane proteins, Biochim. Biophys. Acta 1610 (2003) 57–62.

[87] S.H. Park, F. Casagrande, M. Chu, K. Maier, H. Kiefer, S.J. Opella, Optimization of purification and refolding of the human chemokine receptor CXCR1 improves the stability of proteoliposomes for structure determination, Biochim. Biophys. Acta 1818 (2012) 584–591.

[88] A.A. De Angelis, S.J. Opella, Bicelle samples for solid-state NMR of membrane proteins, Nat. Protoc. 2 (2007) 2332–2338.

[89] J.L. Rigaud, D. Levy, G. Mosser, O. Lambert, Detergent removal by non-polar polystyrene beads, Eur. Biophys. J. 27 (1998) 305–319.

[90] G.A. Signorell, T.C. Kaufmann, W. Kukulski, A. Engel, H.W. Remigy, Controlled 2D crystallization of membrane proteins using methyl-beta-cyclodextrin, J. Struct. Biol. 157 (2007) 321–328.

[91] U. Carraro, D. Doria, C. Rizzi, M. Sandri, A new two-step precipitation method removes free-SDS and thiol reagents from diluted solutions, and then allows recovery and quantitation of proteins, Biochem. Biophys. Res. Commun. 200 (1994) 916–924.

[92] D. Levy, A. Bluzat, M. Seigneuret, J.L. Rigaud, A systematic study of liposome and proteoliposome reconstitution involving Bio-Bead-mediated Triton X-100 removal, Biochim. Biophys. Acta 1025 (1990) 179–190.

[93] W.J. Degrip, J. Vanoostrum, P.H. Bovee-Geurts, Selective detergent-extraction from mixed detergent/lipid/protein micelles, using cyclodextrin inclusion compounds: a novel generic approach for the preparation of proteoliposomes, Biochem. J. 330 (Pt 2) (1998) 667–674.

[94] M. Sandri, C. Rizzi, C. Catani, U. Carraro, Selective removal of free dodecyl sulfate from 2-mercaptoethanol-SDS-solubilized proteins before KDS-protein precipitation, Anal. Biochem. 213 (1993) 34–39.

[95] T.A. Cross, M. Sharma, M. Yi, H.X. Zhou, Influence of solubilizing environments on membrane protein structures, Trends Biochem. Sci. 36 (2011) 117–125.

[96] D. Bavli, M. Tkachev, H. Piwonski, E. Capua, I. de Albuquerque, D. Bensimon, G. Haran, R. Naaman, Detection and quantification through a lipid membrane using the molecularly controlled semiconductor resistor, Langmuir 28 (2012) 1020–1028.

[97] A. Lundquist, S.B. Hansen, H. Nordstrom, U.H. Danielson, K. Edwards, Biotinylated lipid bilayer disks as model membranes for biosensor analyses, Anal. Biochem. 405 (2010) 153–159.

[98] S. Inagaki, R. Ghirlando, R. Grisshammer, Biophysical characterization of membrane proteins in nanodiscs, Methods 59 (2013) 287–300.

[99] A. Nath, W.M. Atkins, S.G. Sligar, Applications of phospholipid bilayer nanodiscs in the study of membranes and membrane proteins, Biochemistry 46 (2007) 2059–2069.

[100] S.H. Park, S. Berkamp, G.A. Cook, M.K. Chan, H. Viadiu, S.J. Opella, Nanodiscs versus macrodiscs for NMR of membrane proteins, Biochemistry 50 (2011) 8983–8985.

[101] A.Z. Kijac, Y. Li, S.G. Sligar, C.M. Rienstra, Magic-angle spinning solid-state NMR spectroscopy of nanodisc-embedded human CYP3A4, Biochemistry 46 (2007) 13696–13703.

[102] Y. Li, A.Z. Kijac, S.G. Sligar, C.M. Rienstra, Structural analysis of nanoscale self-assembled discoidal lipid bilayers by solid-state NMR spectroscopy, Biophys. J. 91 (2006) 3819–3828.

[103] L. Cegelski, REDOR NMR for drug discovery, Bioorg. Med. Chem. Lett. 23 (2013) 5767–5775.

[104] T. Gullion, J. Schaefer, Rotational-echo double-resonance NMR, J. Magn. Reson. 81 (1989) 196–200.

[105] S.J. Opella, Protein dynamics by solid state nuclear magnetic resonance, Methods Enzymol. 131 (1985) 327–361.

[106] S.R. Hartmann, E.L. Hahn, Nuclear double resonance in the rotating frame, Phys. Rev. 128 (1962) 2042–2053.

[107] A. Pines, M.G. Gibby, J.S. Waugh, Proton-enhanced NMR of dilute spins in solids, J. Chem. Phys. 59 (1973) 569–590.

[108] L. Chen, J.M. Kaiser, T. Polenova, J. Yang, C.M. Rienstra, L.J. Mueller, Backbone assignments in solid-state proteins using J-based 3D heteronuclear correlation spectroscopy, J. Am. Chem. Soc. 129 (2007) 10650–10651.

[109] W. Rothwell, J. Waugh, Transverse relaxation of dipolar coupled spin systems under rf irradiation: detecting motions in solids, J. Chem. Phys. 74 (1981) 2721.

[110] D. Suwelack, W. Rothwell, J. Waugh, Slow molecular motion detected in the NMR spectra of rotating solids, J. Chem. Phys. 73 (1980) 2559.

[111] E. Katoh, K. Takegoshi, T. Terao, 13C nuclear Overhauser polarization—magic-angle spinning nuclear magnetic resonance spectroscopy in uniformly 13C-labeled solid proteins, J. Am. Chem. Soc. 126 (2004) 3653–3657.

[112] R. Purusottam, G. Bodenhausen, P. Tekely, Quantitative one- and two-dimensional 13C spectra of microcrystalline proteins with enhanced intensity, J. Biomol. NMR 57 (2013) 11–19.

[113] K. Takegoshi, S. Nakamura, T. Terao, 13C–1H dipolar-assisted rotational resonance in magic-angle spinning NMR, Chem. Phys. Lett. 344 (2001) 631–637.

[114] A. Pines, T. Shattuck, Carbon13-proton NMR cross-polarization times in solid adamantane, J. Chem. Phys. 61 (1974) 1255–1256.

[115] G.A. Morris, Sensitivity enhancement in nitrogen-15 NMR: polarization transfer using the INEPT pulse sequence, J. Am. Chem. Soc. 102 (1980) 428–429.

[116] D. Suter, R. Ernst, Spin diffusion in resolved solid-state NMR spectra, Phys. Rev. B 32 (1985) 5608.

[117] N.M. Szeverenyi, M.J. Sullivan, G.E. Maciel, Observation of spin exchange by two-dimensional fourier transform 13C cross polarization-magic-angle spinning, J. Magn. Reson. 47 (1982) (1969) 462–475.

[118] R.S. Thakur, N.D. Kurur, P. Madhu, Swept-frequency two-pulse phase modulation for heteronuclear dipolar decoupling in solid-state NMR, Chem. Phys. Lett. 426 (2006) 459–463.

[119] A. Shaka, J. Keeler, R. Freeman, Evaluation of a new broadband decoupling sequence: WALTZ-16, J. Magn. Reson. 53 (1983) 313–340.

[120] A. Schuetz, C. Wasmer, B. Habenstein, R. Verel, J. Greenwald, R. Riek, A. Böckmann, B.H. Meier, Protocols for the sequential solid-state NMR spectroscopic assignment of a uniformly labeled 25 kDa protein: HET-s(1–227), ChemBioChem 11 (2010) 1543–1551.

[121] P. Schanda, B.H. Meier, M. Ernst, Accurate measurement of one-bond H-X heteronuclear dipolar couplings in MAS solid-state NMR, J. Magn. Reson. 210 (2011) 246–259.

[122] S.V. Dvinskikh, H. Zimmermann, A. Maliniak, D. Sandstrom, Heteronuclear dipolar recoupling in solid-state nuclear magnetic resonance by amplitude-, phase-, and frequency-modulated Lee–Goldburg cross-polarization, J. Chem. Phys. 122 (2005) 044512.

[123] X. Zhao, M. Edén, M.H. Levitt, Recoupling of heteronuclear dipolar interactions in solid-state NMR using symmetry-based pulse sequences, Chem. Phys. Lett. 342 (2001) 353–361.

[124] M.H. Levitt, D.M. Grant, R.K. Harris, Symmetry-based pulse sequences in magic-angle spinning solid-state NMR, Solid State NMR Stud. Biopolym. (2012) 229.

[125] G. Hou, I.J. Byeon, J. Ahn, A.M. Gronenborn, T. Polenova, 1H-13C/1H-15 N heteronuclear dipolar recoupling by R-symmetry sequences under fast magic angle spinning for dynamics analysis of biological and organic solids, J. Am. Chem. Soc. 133 (2011) 18646–18655.

[126] C.A. Rohl, C.E.M. Strauss, K.M.S. Misura, D. Baker, Protein structure prediction using Rosetta, in: B. Ludwig, L.J. Michael (Eds.), Methods in Enzymology, vol. 383, Academic Press, 2004, pp. 66–93.

[127] R. Das, D. Baker, Macromolecular modeling with Rosetta, Annu. Rev. Biochem. 77 (2008) 363–382.

[128] K.W. Kaufmann, G.H. Lemmon, S.L. DeLuca, J.H. Sheehan, J. Meiler, Practically useful: what the Rosetta Protein Modeling Suite can do for you, Biochemistry 49 (2010) 2987–2998.

[129] V. Yarov-Yarovoy, J. Schonbrun, D. Baker, Multipass membrane protein structure prediction using Rosetta, Proteins: Struct. Func. Bioinforma. 62 (2006) 1010–1025.

[130] P. Barth, J. Schonbrun, D. Baker, Toward high-resolution prediction and design of transmembrane helical protein structures, Proc. Natl. Acad. Sci. 104 (2007) 15682–15687.

[131] T.A. Jones, S. Thirup, Using known substructures in protein model building and crystallography, EMBO J. 5 (1986) 819–822.

[132] A. Cavalli, X. Salvatella, C.M. Dobson, M. Vendruscolo, Protein structure determination from NMR chemical shifts, Proc. Natl. Acad. Sci. 104 (2007) 9615–9620.

[133] Y. Shen, O. Lange, F. Delaglio, P. Rossi, J.M. Aramini, G. Liu, A. Eletsky, Y. Wu, K.K. Singarapu, A. Lemak, A. Ignatchenko, C.H. Arrowsmith, T. Szyperski, G.T. Montelione, D. Baker, A. Bax, Consistent blind protein structure generation from NMR chemical shift data, Proc. Natl. Acad. Sci. 105 (2008) 4685–4690.

[134] C.A. Rohl, D. Baker, De novo determination of protein backbone structure from residual dipolar couplings using Rosetta, J. Am. Chem. Soc. 124 (2002) 2723–2729.

[135] M.J. Berardi, W.M. Shih, S.C. Harrison, J.J. Chou, Mitochondrial uncoupling protein 2 structure determined by NMR molecular fragment searching, Nature 476 (2011) 109–113.

[136] O.F.L.S. Raman, P. Rossi, M. Tyka, X. Wang, J. Aramini, G. Liu, T.A. Ramelot, A. Eletsky, T. Szyperski, M.A. Kennedy, J. Prestegard, G.T. Montelione, D. Baker, NMR structure determination for larger proteins using backbone-only data, Science 327 (2010) 5.

[137] G. Cornilescu, F. Delaglio, A. Bax, Protein backbone angle restraints from searching a database for chemical shift and sequence homology, J. Biomol. NMR 13 (1999) 289–302.

[138] Y. Shen, F. Delaglio, G. Cornilescu, A. Bax, TALOS+: a hybrid method for predicting protein backbone torsion angles from NMR chemical shifts, J. Biomol. NMR 44 (2009) 213–223.

[139] R.S. Prosser, S.A. Hunt, J.A. DiNatale, R.R. Vold, Magnetically aligned membrane model systems with positive order parameter: switching the sign of Szz with paramagnetic ions, J. Am. Chem. Soc. 118 (1996) 269–270.